

Closed-Loop Control of Plasma Osmolality in Patients with Central Diabetes Insipidus

Kamel Zaarouri



Department of Electrical & Computer Engineering
McGill University
Montreal, Canada

February 2010

A thesis submitted to McGill University in partial fulfillment of the requirements for the degree of Masters in Electrical Engineering.

© 2010 Kamel Zaarouri

Abstract

Central Diabetes Insipidus is a disorder that is characterized by decreased secretion of a certain hormone in the human body called the antidiuretic hormone (ADH). Patients affected with central diabetes insipidus will have an abnormally high *plasma osmolality* level manifested by a reduced ability to concentrate urine, excessive thirst and excessive urine production [1].

Currently, Central Diabetes Insipidus is treated by administering synthetic ADH as a nasal spray. In this thesis, a closed-loop automated treatment system has been investigated. For that end, advanced control techniques were studied, from a *Smith Predictor* to \mathcal{H}_∞ *Optimal Control* and *Robust Control*. The effectiveness of the controllers to reject a step disturbance in the plasma osmolality was examined. This Thesis shows the potential use of control theory in the context of Central Diabetes Insipidus.

Abrégé

Le *Diabète Insipide Central* est un désordre qui est caractérisé par la sécrétion diminuée d'une certaine hormone dans le corps humain appelé l'hormone antidiurétique (ADH). Les patients affectés par cette anomalie auront un taux anormalement élevé d'*osmolalité du plasma*, manifesté par une diminution de la concentration de l'urine et par un excès de soif et de production d'urine.

Actuellement, on traite le Diabète Insipide Central en administrant de l'ADH synthétique avec un vaporisateur nasal. Dans cette thèse, un système de traitement automatisé a été étudié. À cette fin, des techniques de contrôle avancées ont été étudiées, à savoir le *Prédicteur de Smith*, la commande *Optimale \mathcal{H}_∞* et la commande *Robuste*. L'efficacité des contrôleurs pour minimiser l'effet des perturbations en échelon dans l'*osmolalité du plasma* a été examinée. Entre-autre, cette Thèse montre l'utilisation potentielle de la théorie de contrôle dans le contexte du Diabète Insipide Central.

Acknowledgments

First and Foremost, I would like to thank my professor and supervisor, Prof. Benoit Boulet whom I have had the pleasure of working with him for almost two years. This thesis would not have been possible without him. One could not wish for a better, friendlier and kindlier supervisor.

I am much grateful to Ph.D. Candidate Mr. Ahmad Haidar, who proved to be a dear friend and colleague since the start of my graduate education. His advice and experience enabled me to develop a deep and thorough understanding of the *Systems and Control* subject and in writing this thesis. I owe much gratitude to Mr. Haidar, my Masters studies at McGill University will always be marked by him.

In my daily work I have been blessed with a friendly and helpful group of fellow students, Ph.D. Candidates Vahid Raissi Dehkordi, Hamed Azarnoush and Amir Danak, who never hesitated in answering my sometimes lengthy questions despite of their busy schedules.

I would also like to thank Prof. Elizabeth Jones, Assistant Professor in the department of Chemical Engineering; her advice and experience are greatly appreciated.

Lastly, I offer my deepest regards, love and blessings to my family and friends who supported me in many different aspects during the completion of this thesis.

Kamel Zaarouri.

Contents

1	Introduction	1
1.1	Control Theory	1
1.2	Biomedical Applications of Control Theory	2
1.3	Problem Statement and Aim	2
2	Background and Problem Formulation	4
2.1	Plasma Osmolality	5
2.2	Central Diabetes Insipidus	9
2.2.1	Causes and Symptoms	9
2.2.2	Current Treatment	9
2.3	Problem Formulation	10
2.4	Methodology and Contribution	11
3	Literature Review	13
3.1	PID with a Smith Predictor	14
3.2	\mathcal{H}_∞ Optimal Control	14
3.3	Robust Control	15
4	Mathematical Model	16

4.1	Non-Linear Model	16
4.2	LTI-Model	20
5	Smith-predictor	26
5.1	Nyquist Stability Criterion	26
5.2	Smith-Predictor - The Theory	27
5.3	Smith-predictor - Design and Simulations	32
6	\mathcal{H}_∞ Optimal Control	37
6.1	\mathcal{H}_∞ - The Theory	37
6.2	\mathcal{H}_∞ - Design and Simulations	44
7	Robust Control	49
7.1	Uncertainty Modeling and Robust Control Theory	50
7.1.1	Unstructured Uncertainty and The Small Gain Theorem	50
7.1.2	Structured Uncertainty and The Structured Singular Value	53
7.2	Robust Performance	55
7.3	Robust Control - Design and Simulation	55
8	Conclusion	62
8.1	Controller's Effectiveness	62
8.2	Conclusion and Future Work	64
	References	68

List of Figures

2.1	The anatomy of the hypothalamus and pituitary gland depicting the route for ADH secretion. Photo taken from [2] with permission.	6
2.2	The action of ADH in the collecting tubule, increasing water permeability. Figure taken with permission from [3].	7
2.3	The Regulation of plasma osmolality by ADH (The Figure is based on the one present in [3]).	8
2.4	The osmo-regulatory feedback closed-loop system with a compensator, a system model, and a sensing delay of 30 min.	12
4.1	Block diagram describing the non-linear relation between blood ADH concentration and plasma osmolality. OWU is the urine output, VEC is the extracellular fluid volume and OSMP is the plasma osmolality.	16
4.2	The relationship of plasma ADH (AVP) to plasma osmolality OSMP in normal subjects. Figure was taken from [4] with permission.	17

4.3	A block diagram of the human renal system consisting of seven blocks, to the left side of each block there is the inputs, the outputs of the blocks are on the right, and on the top and bottom are the constant parameters and independent inputs and outputs. This figure is taken from [5] with permission.	18
4.4	The simulink model of the relation between blood ADH concentration and plasma osmolality.	19
4.5	Simulink model of the setup used for system identification.	20
4.6	Graphs describing the non-linear model output compared with the obtained LTI model's output subject to white noise of mean one and their relative error.	24
4.7	Graphs describing the behavior of the non-linear model and the LTI model subject to different step changes in the ADH input.	25
5.1	The Nyquist diagram for $G_{OL}(s) = \frac{1}{2s+1}$ with $\mathcal{R}e(G(jw))$ on the x-axis and $\mathcal{I}m(G(jw))$ on the y-axis.	27
5.2	The Nyquist diagram of the open-loop transfer function $G_{OL}(s) = \frac{\mathcal{K}e^{-\phi s}}{\tau s+1}$ for different values of \mathcal{K} . \mathcal{K}_c designates the critical controller gain that render the closed-loop system unstable.	29
5.3	A closed-loop system comprising of a controller, a plant and a deadtime with respective transfer functions $K(s)$, $P(s)$ and $T_d(s)$	30
5.4	The smith-predictor as an improved configuration for dead-time compensation purposes.	30
5.5	The conventional smith-predictor configuration.	31
5.6	Simulink model of the closed-loop osmo-regulatory system utilizing a PD controller.	32

5.7	The response of the omso-regulatory closed-loop system to an output step disturbance of 20 mOsm/l. The Controller used is a PD controller with fixed derivative gain of 0.7 and a varying proportional gain k_p . The output of the controller is also shown for each case.	33
5.8	Simulink model of the closed-loop osmoregulatory system utilizing a PD controller in a smith-predictor configuration.	34
5.9	The response of the omso-regulatory closed-loop system to an output step disturbance of 20 mOsm/l. The Controller used is a PD controller in a smith-predictor configuration, with fixed derivative gain of 0.7 and a varying proportional gain k_p . The output of the controller is also shown for each case.	35
6.1	A SISO feedback system where P and K designate the plant's and controller's transfer function. s and y designate the input and output of the system respectively. respectively	39
6.2	A SISO feedback system showing different weighting functions added at different locations to achieve different control objectives.	41
6.3	Standard system configuration for an H-infinity problem.	42
6.4	The augmented plant P, showing the internal configuration and weighting functions.	43
6.5	The performance objectives defined by the weighting function W_e	46
6.6	The bode plot of the \mathcal{H}_∞ optimal controller.	47
6.7	The response of the Omsoregulatory closed-loop system to an output step disturbance of 20 mOsm/l. The controller used is the \mathcal{H}_∞ optimal controller K . Lastly, the output of the controller is shown.	48
7.1	The additive uncertainty system configuration.	50

7.2	The output multiplicative uncertainty system configuration.	51
7.3	The input multiplicative uncertainty system configuration.	51
7.4	The standard LFT configuration.	52
7.5	The standard M- Δ configuration.	52
7.6	The bode plot of the percentage of the multiplicative model uncertainty. .	56
7.7	The Simulink's nonlinear osmoregulatory system.	58
7.8	Plots of the open-loop response of the perturbed system $G_{p(s)parametric}$ (above) subject to a rectangular pulse at time $t = 400min$ (below).	58
7.9	The upper and lower bound of μ , its actual value lies between these upper and lower bounds.	60
7.10	The Osmoregulatory perturbed system's response to a step output disturbance of 10 mOsm/l at time=10 min. 10 different perturbation system's states were picked randomly.	61
8.1	Plots comparing the responses of the osmoregulatory closed-loop system when the four types of controllers are used: PD, PD in a Smith Predictor Configuration, \mathcal{H}_∞ Controller and Robust Controller subject to an output step disturbance of 10 mOsm/l. 10 random perturbed model instances are used. These plots represent deviation plots, i.e. 0 mOsm/l is equivalent to 287 mOsm/l.	63

-
- 8.2 Comparison of the Settling Time and Peak ADH of the osmoregulatory closed-loop system when the four types of controllers are used: PID, PID in a Smith Predictor Configuration, \mathcal{H}_∞ Controller and Robust Controller subject to an output step disturbance of 10 mOsm/l. 10 random perturbed model instances are used. When the PID controller either in a Smith Predictor configuration or not is used, a saturation block of 0.8 was added on their output. 65
- 8.3 comparing the Settling Time and Peak ADH of the osmoregulatory closed-loop system when the four types of controllers are used: PID, PID in a Smith Predictor Configuration, \mathcal{H}_∞ Controller and Robust Controller subject to an output step disturbance of 10 mOsm/l. 10 random perturbed model instances are used. No saturation blocks were added in this case. 67

Chapter 1

Introduction

1.1 Control Theory

Over the years, control theory became indisputably a central part of any field of engineering and science. Automatic control of systems is driving technology forward, making any machine, process or plant in the broadest of terms function as desired. One of the first significant contribution in automatic control was the one of James Watt who tried to control the speed of a steam engine in the eighteenth century. Soon after, proper mathematical control theory started to be formulated. With scholars like Nyquist (1932) who developed a procedure for determining the stability of closed-loop system, to Bode (1940) who initiated frequency-response analysis of systems; it did not take long for control theory to become the basis for any industrial advancement. From air-conditioning systems that revolutionized living standards by accurately maintaining temperatures of desired environments within certain bounds [6], to automotive control of engines and drivelines [7] that became an everyday reality in transportation systems, automation is now omnipresent within our society.

1.2 Biomedical Applications of Control Theory

Recently, application of such theory in biomedical systems started to emerge. The human body is the ultimate controller, in the sense that it is trying to prevent wide oscillations in the body's internal conditions by keeping any disturbance in the body within narrow limits. *Homeostasis* is a key word that signify the maintenance of this constant internal consistency. With the growing advancements in control theory and algorithms, their application in biological systems was a natural step forward with a twofold motivation. The control and systems theory could be applied from a biomedical aspect to understand how the body can attain homeostasis and from a human aspect by trying to develop methods that help achieve specific homeostasis conditions in patients incapable of doing so.

Biomedical control devices started to emerge rapidly, especially after multiple advancements in nano-technology and computational speeds. Examples worth mentioning of automation application in medicine are artificial heart valves [8], insulin pumps [9], and pacemakers with more than 300,000 implanted per year in the United States alone [10].

1.3 Problem Statement and Aim

Central diabetes insipidus (CDI) is a rare hypothalamus-pituitary disorder that is characterized by decreased secretion of the antidiuretic hormone (ADH) in the human body. Patients affected with CDI will have an abnormally high *plasma osmolality* level manifested by a reduced ability to concentrate urine, excessive thirst and excessive urine production [1].

Currently, CDI is treated in an open-loop fashion by administering a synthetic ADH as a nasal spray. In this Thesis, we will be investigating the possibility of a closed-loop regulation of the plasma osmolality level in patients affected with CDI. In this type of

control, patient's manual intervention is eliminated, an automated regulatory system will allow them to live a high quality life similar to that of a healthy subject.

Chapter 2

Background and Problem

Formulation

Cells are the building blocks of our body, combining to form anything from tissues to organs. All cells swim in a liquid called tissue fluid [11]. This fluid supported by the blood, supplies cells with nutrients and form the necessary environment that each cell needs to perform its specific function. Although in the body there are trillions of specific cells, each looking for its own optimum condition, the body acts as a whole regulating the conditions for healthy growth and efficient functioning of the cells.

The Environmental factors affecting cellular activity are:

- Plasma Osmolality(OMSP)
- Temperature
- Hydrogen-ion concentration

Any disruption of the homeostatic level of any of those items will be destructive to the cells.

2.1 Plasma Osmolality

Plasma Osmolality (OSMP) is a key environmental factor affecting cellular activity, it is estimated in [2] by:

$$OSMP = 2(Plasma [Na^+]) + \frac{[Glucose]}{18} + \frac{[BUN]}{2.8}, \quad (2.1)$$

where plasma osmolality (OSMP) as well as the plasma concentration of Sodium (Plasma[Na⁺]) are expressed in mOsm/l¹. The [Glucose] and [BUN] (Blood Urea Nitrogen) concentrations are expressed in mg/dl (the division by 18 for the glucose and 2.8 for the BUN allows conversion from mg/dl to mOsm/l).

OSMP is strictly maintained at constant level within the body and any variation of its concentration in either directions of about 3 mOsm/l will result in the stimulation of the body's osmolality regulating mechanisms. The alterations of the OSMP are detected by osmoreceptors in the vicinity of the supraoptic and paraventricular areas of the hypothalamus (Figure 2.1). These receptors regulate the release of the antidiuretic hormone (ADH) also known as vasopressin [3].

¹osmole (with symbol Osm) is a unit of osmotic pressure equivalent to the amount of solute that dissociates in solution to form one mole (Avogadro's number) of particles (molecules and ions). (Definition taken directly from [12])

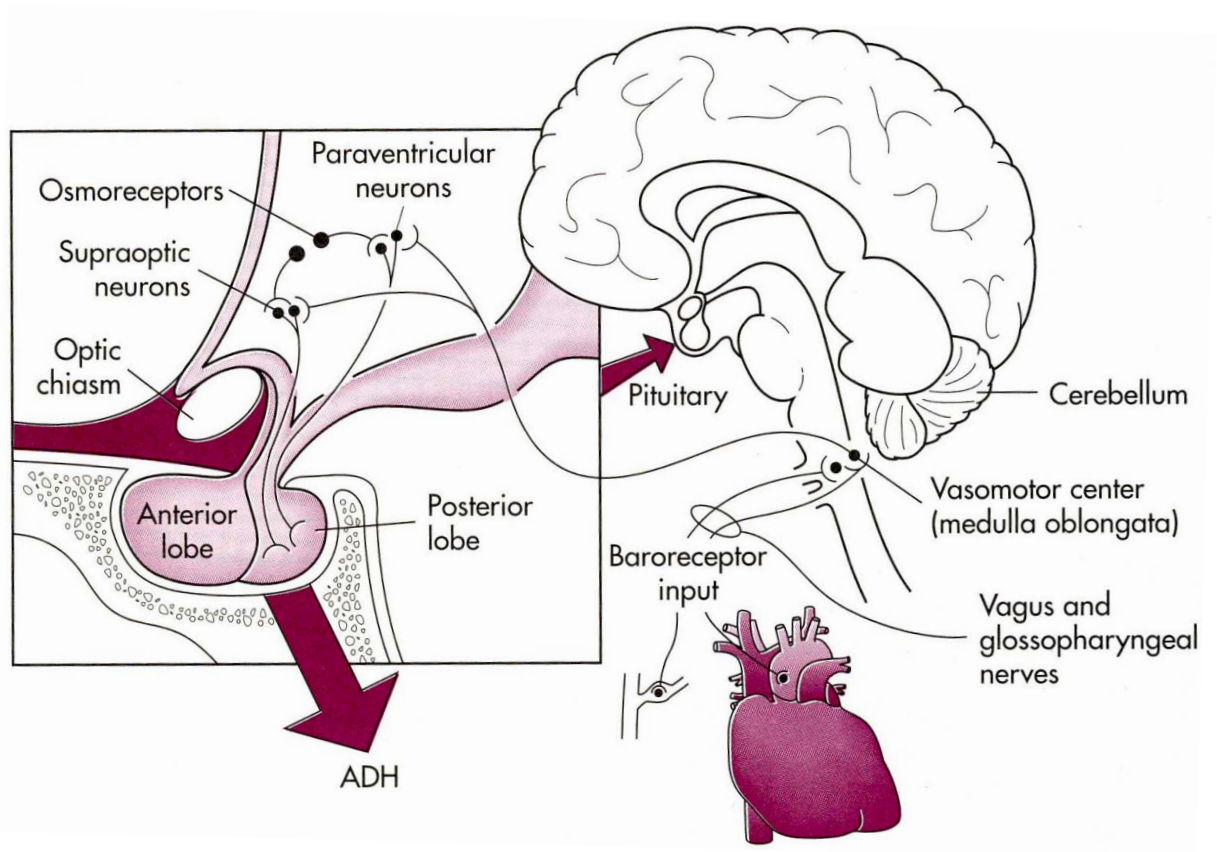


Fig. 2.1 The anatomy of the hypothalamus and pituitary gland depicting the route for ADH secretion. Photo taken from [2] with permission.

Cellular dehydration occurs when extracellular fluid osmolality is increased relative to that of the intracellular fluids. The relationship between the OSMP and the plasma ADH concentration is such that at normal OSMP level (about 287 mOsm/l) there is ADH present in the plasma; lowering the OSMP reduces the plasma ADH concentration and raising the OSMP increases the plasma ADH concentration [1].

When extra-cellular fluid (ECF) osmolality increases, the osmoreceptors shrink and release ADH [13]. ADH markedly increases water re-absorption in renal collecting tubules, which will reduce OSMP to normal again (Figure 2.2). Conversely, a decrease in ECF osmolality, will inhibit the release of ADH in the blood stream, decreasing water re-absorption in renal collecting tubules and consequently regulating OSMP to homeostatic levels. Figure 2.3 shows a diagram describing this osmo-regulatory mechanism.

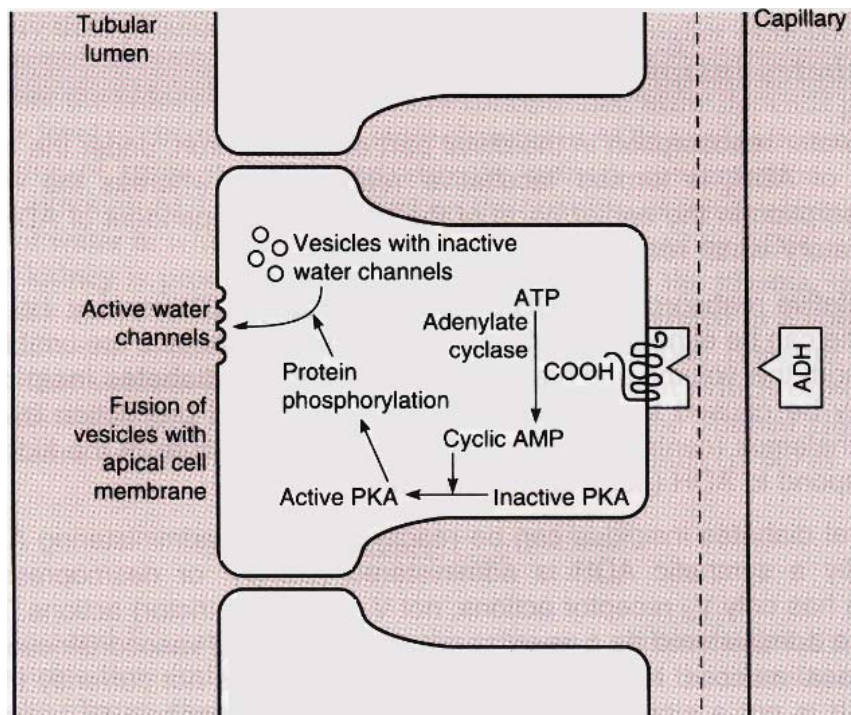


Fig. 2.2 The action of ADH in the collecting tubule, increasing water permeability. Figure taken with permission from [3].

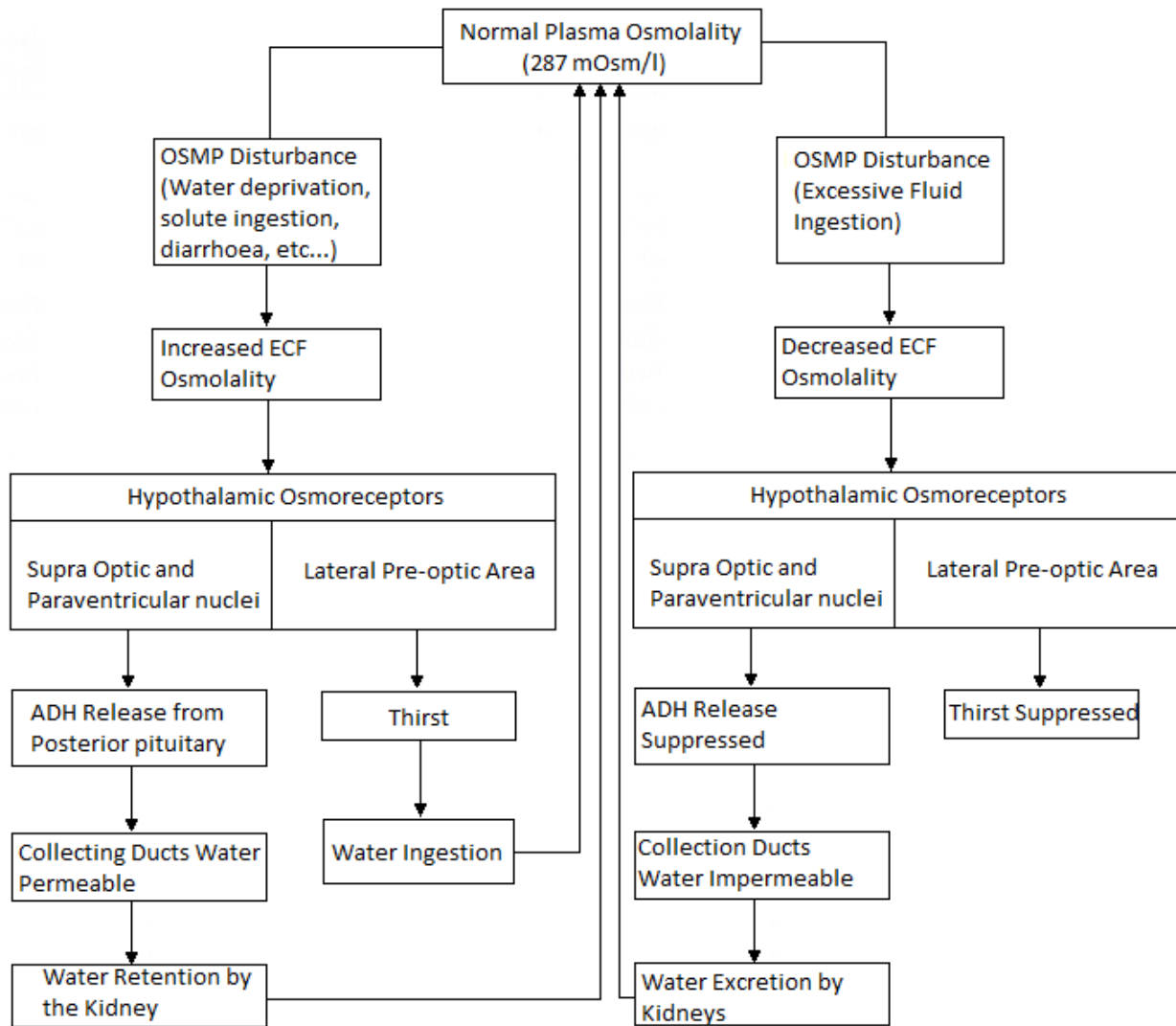


Fig. 2.3 The Regulation of plasma osmolality by ADH (The Figure is based on the one present in [3]).

2.2 Central Diabetes Insipidus

Central diabetes insipidus (CDI) is a syndrome that affects the body's ability to conserve water and is characterized by the decreased secretion of the antidiuretic hormone. Patients affected with CDI will have reduced ability to concentrate urine and consequently maintain healthy Plasma Osmolality levels [1].

2.2.1 Causes and Symptoms

Central diabetes insipidus results from the inhibited production of the antidiuretic hormone. This could be due to a variety of reasons. The disorder may be caused by damage of the hypothalamus; a tumor; interruption of blood supply, due to some sort of a blockage in the arteries leading to the brain; a brain injury; a trauma; or even genetic. How complete CDI is, depends on the extent of the damage [14].

The usual symptoms of CDI are intense thirst (with a special craving for ice-cold water) and excessive urine production. A person affected with CDI will drink large amounts of fluids, anywhere from 3 to 30 liters per day to compensate for the fluid lost in urine. The inability to compensate the fluid losses can result in low blood pressure and shock [15].

2.2.2 Current Treatment

Currently, OSMP in patients with CDI is regulated in an open-loop fashion by administering a synthetic ADH. In this type of treatment, any momentary disturbance of the normal osmolality levels will not be corrected until the next scheduled administration of the prescribed medication, causing frequent and significant OSMP variations.

Vasopressin or desmopressin (DDAVP) (1-desamino-8-arginine vasopressin) is a synthetic analog of the human antidiuretic hormone (ADH) which was produced in 1966 by

removing an amino group from the cysteine molecule in position 1 and replacing a residue of L-arginine with D-arginine in position 8 [16]. DDAVP is an effective drug against CDI and is usually administered as a nasal spray. Desmopressin is considered a safe drug, unfortunately improper administered amounts can lead to fluid retention, swelling, and other problems, rare but serious effect of desmopressin overdose is water intoxication [17].

2.3 Problem Formulation

In this thesis, we will be investigating the possibility of a closed-loop regulation of the plasma osmolality level in patients affected with central diabetes insipidus. This regulatory system will have to contain three major components (Figure 2.4): A plasma osmolality sensor, a mechanical pump capable of delivering the synthetic ADH and a control algorithm to regulate the pump's action.

Sodium (Na^+) and BUN (Blood Urea Nitrogen) implantable sensors have been readily available in the market for over 10 years with a measurement delay of few milliseconds. With implantable glucose sensors currently being developed to automatically measure interstitial glucose every few minutes [18], an OSMP sensor can be put together with a total sensing delay of that of the glucose's. Furthermore, significant work has been done to develop piezoresistive embedded osmolality sensors that could measure accurately plasma osmolality [19]. The reliability of such devices continues to increase.

If the osmolality sensor is implanted directly into the blood stream, the delay between any disturbance in the osmolality and the measurements would be in the order of few minutes. Unfortunately, biomedical sensors for safety reasons cannot be implanted directly in the blood stream and any measurement of the blood stream's biological analytes has to be done indirectly in the interstitial fluid (ISF). Therefore, any disturbance in the plasma

composition will be kept undetectable in the ISF for about 25 min; When adding to that the delay of the OSMP sensor, any measurement of the OSMP from the ISF will then have a delay of about 30 min. Therefore, any control strategy would have to be tested in the presence of that inherent delay.

Implantable pumps for drug delivery systems has been in service for over 25 years. Insulin pumps are a good example of such systems [20, 21]. Work is now being done on high-performance silicon implantable micropumps, with accurate pumping characteristics and intrinsic insensitivity to external condition [22].

2.4 Methodology and Contribution

To the best of our knowledge, no prior work has been done on any form of closed-loop regulation of OSMP in patients with CDI. In this thesis, we start by giving some background information about central diabetes insipidus, causes and current treatment methodologies; we will then continue by doing some literature review; then proceed in deriving an LTI model for the renal/body fluid system, specifically the system describing the *Osmoregulatory* renal function; finally, we will study different control strategies starting with *PID* control, \mathcal{H}_∞ optimal control then *Robust Control* and conclude by discussing their performance. The primitive Osmoregulatory feedback control system will look like the one shown in Figure 2.4.

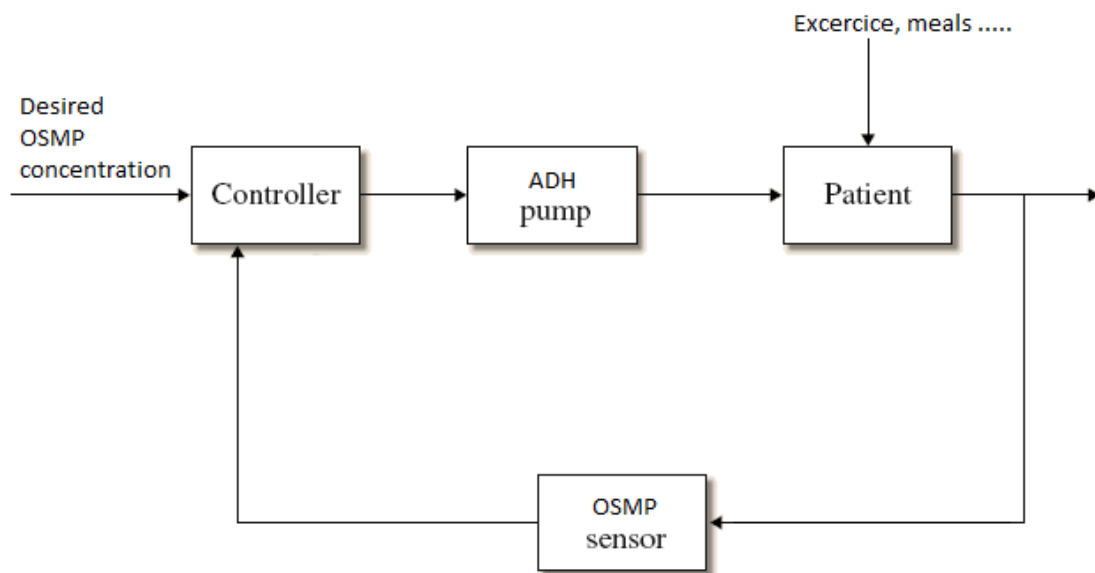


Fig. 2.4 The osmo-regulatory feedback closed-loop system with a compensator, a system model, and a sensing delay of 30 min.

Chapter 3

Literature Review

Many mathematical models of the renal/body fluid system has been previously developed. Guyton et al. [23] was a pioneer in deriving a detailed model of the Renal function from a system analysis point of view. Uttamsingh et al. [24] presented an overall representation of the renal/body fluid system with an emphasis on the undergoing control mechanisms. On the other hand, many models of the renal/body fluid system have been developed to highlight specific features of the control system, like Merletti and Weed [25] who investigated a relatively complete non-linear model of fluid volume and osmolality control systems in the human body. Others, like G. Ciofani et al. [26], derived a simpler linear model to describe plasma osmolality control in the kidney.

The model of the renal system used in this thesis is based on the one derived by Noraki Ikeda et al. [5] who built a biological system model capable of reproducing clinical findings and measurements.

3.1 PID with a Smith Predictor

Despite the considerable development of advanced control theory and the availability of industrial controllers (PLC's) capable on implementing the algorithms; Proportional-Integral-Derivative (PID) controllers are still extensively used in the industry since their first appearance in the 1940's. This is due to the fact that PID controllers are known to have satisfactory performance in a wide range on processes and robustness over a wide range of operating conditions on top of being easily implementable.

However, systems with long time-delays (or dead-time) can only be stabilized by decreasing the controller's gain, resulting in a sluggish response [27]. Consequently, a *Smith Predictor* was the industry's answer to those type of plants due to its effective dead-time compensation capabilities [28]. Although the Smith-Predictor is nominally stable, it's performance is highly dependent on the accuracy of the plant's model, any model uncertainty or perturbation in the plant's dynamics can easily destabilize the feedback system [29].

3.2 \mathcal{H}_∞ Optimal Control

\mathcal{H}_∞ optimal control theory addresses the issue of worst-case controller design for linear systems subject to disturbances. \mathcal{H}_∞ optimal control seeks to bound the energy gain of the system [30]. However, optimal control algorithms are designed to perform under nominal conditions and they are not always tolerant to uncertainties in the system or the environment.

3.3 Robust Control

Any operational control system has to have three properties, stability, controllability and observability. One definition of stability is referred to as BIBO stability, i.e. for each bounded input to the system there is a bounded output. Controllability is the ability to control (transfer) any given state in the system to the origin. Observability is the ability to observe all states of the system. Maintaining all three properties is crucial for the success of any control system. Unfortunately, uncertainties in the system makes it difficult to attain these properties due to the limited information the system's engineer has in hand. "Robust control refers to the control of unknown plants with unknown dynamics subject to unknown disturbances" [30]. This type of control tries to bound the frequency response of the uncertainties and build a compensator that is stable and capable on performing under any operating conditions within the set bound.

Robust control theory is based on extensive work done by Zames (1965), more specifically regarding the small gain and circle theorem. The early robust control work was emphasized on formulating sufficient condition for stability of uncertain systems with a single norm bound (unstructured uncertainty). It then became clear that stability conditions for this type of uncertainties was too conservative and restrictive for numerous applications. These methods were based on singular values of matrices. Freudenberg et al. [31] proposed that something more was needed. Soon after, Safonov [32] introduced the concept of a structured uncertainty, and it was not until Doyle [33] that the problem of robust performance with structured uncertainty was explicitly formulated and solved.

Chapter 4

Mathematical Model

4.1 Non-Linear Model

Noraki Ikeda et al. [5] built a complete renal system model capable of reproducing clinical findings and measurements. This complete model is shown in Figure 4.3. Based on this model, we were able to derive a model of the *Osmoregulatory* system that describes the non-linear relation between blood ADH concentration and plasma osmolality, Figures 4.1,4.4.

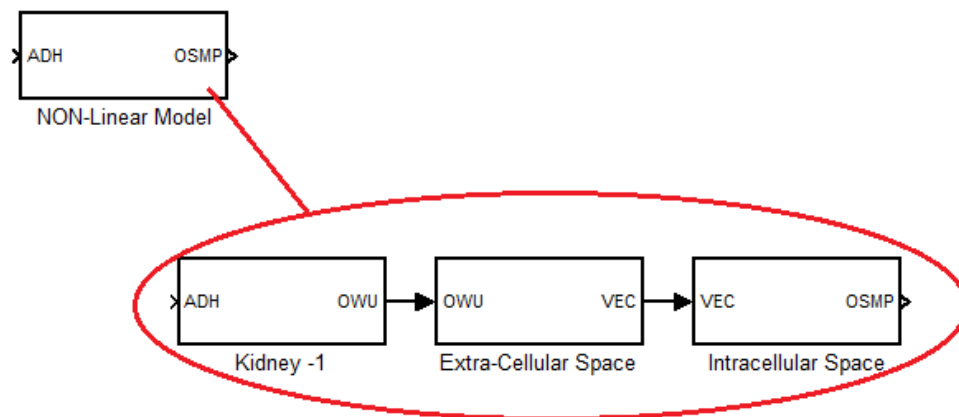


Fig. 4.1 Block diagram describing the non-linear relation between blood ADH concentration and plasma osmolality. OWU is the urine output, VEC is the extracellular fluid volume and OSMP is the plasma osmolality.

In this model, ADH is expressed as the ratio to the normal (or nominal) homeostasis level. This choice of a normalized variable was not arbitrary, since as seen from Figure 4.2 the nominal ADH level even for a specific nominal OSMP concentration of 287 mOsm/l can vary 500% from 1 to 5 pg/ml depending on the individual. Thus, in case of existence of such device that would control OSMP in patients with CDI, a prior study regarding the nominal value of ADH of each CDI patient has to be determined.

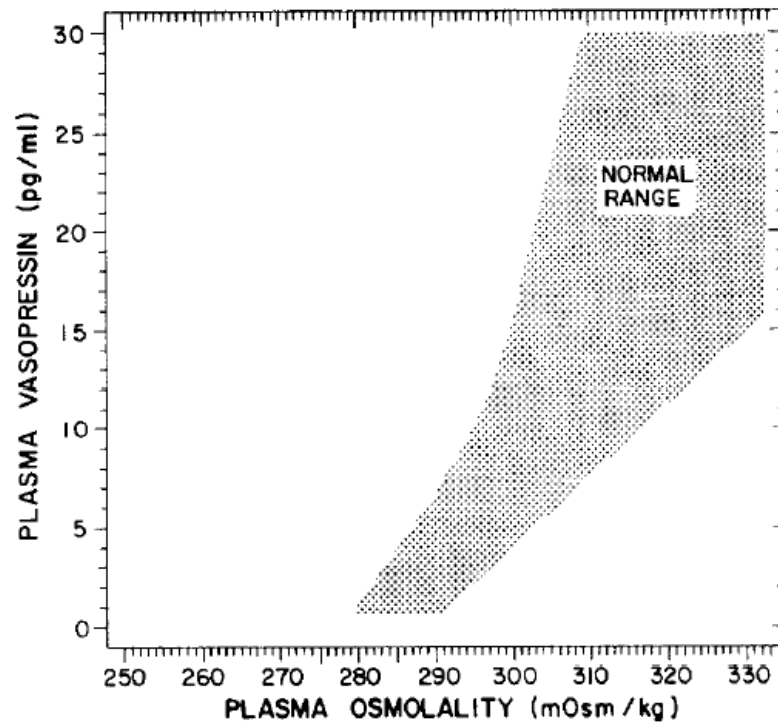


Fig. 4.2 The relationship of plasma ADH (AVP) to plasma osmolality OSMP in normal subjects. Figure was taken from [4] with permission.

4.2 LTI-Model

We then proceeded in linearizing the model. Unfortunately, because of the complexity of the system, linearizing from input/output equations turned out to be a very complex task. Consequently, *Small Signal (SS) Model Identification* technique was used. The obtained small signal linear model is stable and fairly accurate around an equilibrium point, which is usually taken to be the operating point of the non-linear system. Since, the LTI model will be in a closed loop feedback configuration that will maintain the system around that equilibrium point; The SS linear model is a valid one for our objectives.

The strategy now is to determine the equilibrium point of the non-linear system and to linearize around it. The equilibrium point is defined as the state that the system would remain in under nominal conditions, subject to no external perturbations. The operating point of the studied non-linear system is an input of ADH= 1 that will maintain a nominal constant plasma osmolality level of 287 mOsm/l.

Consequently, as seen in Figure 4.5, the system was stimulated with a Gaussian noise of mean zero around the operating point. I/O data were recorded and processed for system identification purposes.

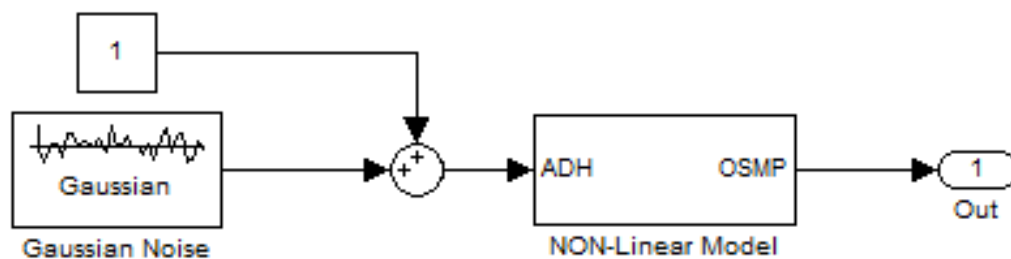


Fig. 4.5 Simulink model of the setup used for system identification.

The ARMAX estimator in Matlab's system identification toolbox was then used. The following definition of the ARMAX model is extracted directly from Matlab's Help:

$$y(t) + a_1y(t-1) + \dots + a_{n_a}y(t-n_a) = \\ b_1u(t-1) + \dots + b_{n_b}u(t-n_b) + e(t) + c_1e(t-1) + \dots + c_{n_c}e(t-n_c)$$

where,

- $y(t)$ is the output at time t .
- $a_1\dots a_n$, $b_1\dots b_n$ and $c_1\dots c_n$ are the parameters to be estimated.
- n_a is the number of poles of the system.
- $n_b - 1$ is the number of zeros of the system.
- n_c is the number of previous error terms on which the current output depends.
- n_k is the number of input samples that occur before the inputs affecting the current out.
- $y(t-1)\dots y(t-n_a)$ are the previous outputs on which the current output depends.
- $u(t-n_k)\dots u(t-n_k-n_b+1)$ are the previous inputs on which the current output depends.
- $e(t), e(t-1), \dots, e(t-n_c)$ are the white-noise disturbance values on which the current output depends.

Using the ARMAX estimator and with respective coefficients $(n_a, n_b, n_c, n_k) = (3, 3, 3, 1)$; we were able to approximate with a fit of 97.4% the 11th order non-linear system with a 3rd order LTI system¹ with transfer function:

$$G(s) = \frac{-0.2283s^2 - 0.01486s - 0.001346}{s^3 + 0.06588s^2 + 0.006106s + 3.591 \times 10^{-7}}.$$

Consider the following state-space representation of the model:

$$\begin{aligned}\dot{\mathbf{x}} &= A\mathbf{x} + Bu \\ y &= C\mathbf{x} + Du\end{aligned}$$

where u is the ADH concentration expressed as the ratio to the normal level, y the OSMP expressed in mOsm/l and \mathbf{x} is the vector state of the system.

The $\left[\begin{array}{c|c} A & B \\ \hline C & D \end{array} \right]$ matrices were then derived, completing the continuous-time state-space representation of the model:

$$A = \begin{bmatrix} & x_1 & x_2 & x_3 \\ x_1 & 7.478 & 2.511 & -2.522 \\ x_2 & -9.956 & -0.02196 & 10.04 \\ x_3 & 2.478 & -2.489 & -7.522 \end{bmatrix}, B = \begin{bmatrix} u_1 \\ x_1 & -0.2283 \\ x_2 & 0.4535 \\ x_3 & -0.2253 \end{bmatrix}$$

¹The obtained system was in the digital domain, consequently Matlab's d2c command was then used to convert it to continuous time.

$$C = \begin{bmatrix} & x_1 & x_2 & x_3 \\ y_1 & 1 & 0 & 0 \end{bmatrix}, D = \begin{bmatrix} & u_1 \\ y_1 & 0 \end{bmatrix}$$

Figure 4.6 shows the non-linear model output when compared with the derived LTI model's output subject to white noise of mean one². We chose white noise as input due to its *flat* spectrum thus stimulating the models over all frequencies.

Having an almost matching output under white noise input as seen in Figure 4.6 confirms the validity of the 3rd order LTI model.

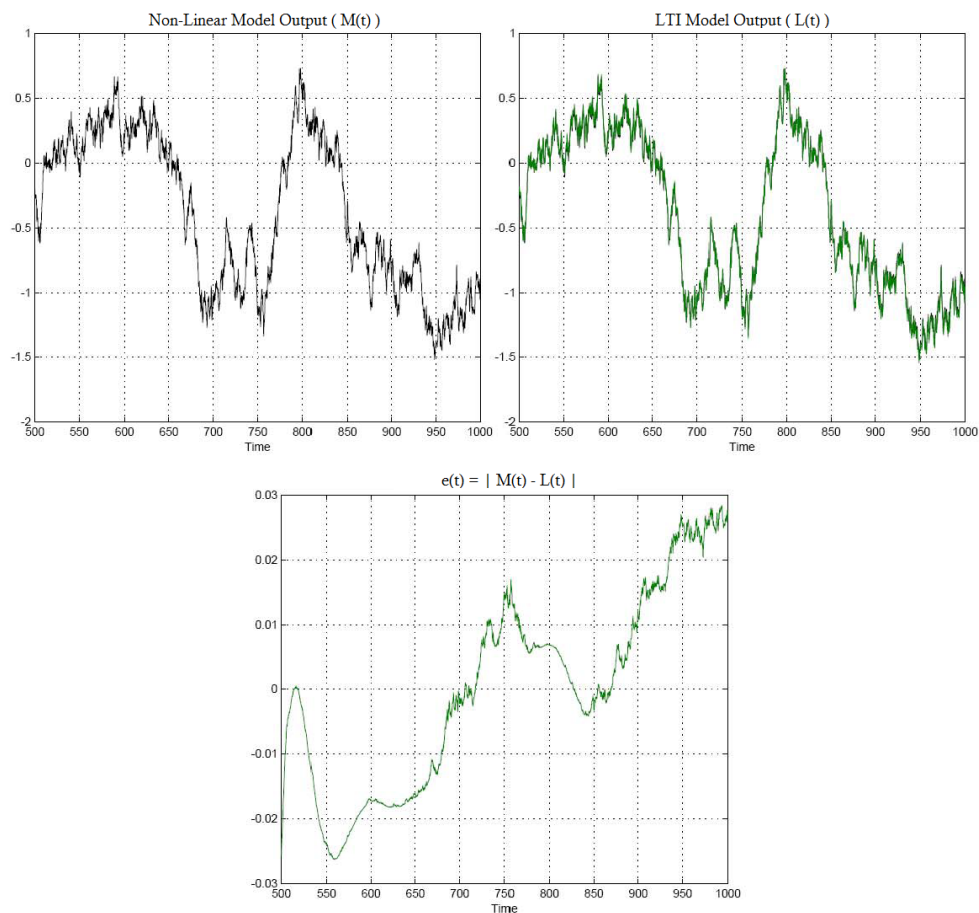


Fig. 4.6 Graphs describing the non-linear model output compared with the obtained LTI model's output subject to white noise of mean one and their relative error.

²The stimulus (white noise) used here is different from the one used for the fitting algorithm

Figure 4.7 is a comparison of the behavior of the non-linear model and the LTI model obtained by system identification subject to different step changes in the ADH.

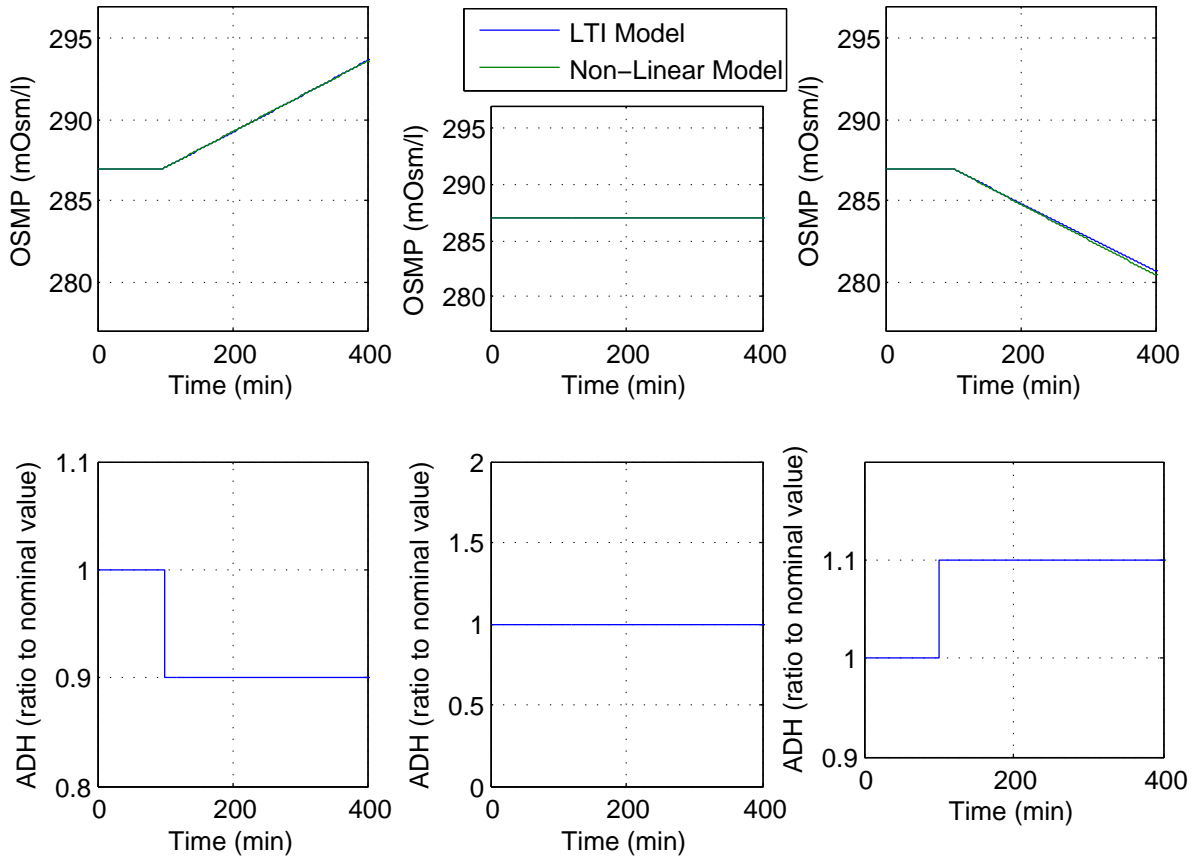


Fig. 4.7 Graphs describing the behavior of the non-linear model and the LTI model subject to different step changes in the ADH input.

The derived LTI model will approximate the non-linear model around its operating point. The linear model will have an operating point of zero that will correspond to an ADH input of 1 and a nominal output of zero that will correspond to a OSMP concentration of 287 mOsm/l.

Now, with the LTI model complete, we were then able to proceed in deriving controllers for the closed-loop Osmoregulatory system.

Chapter 5

Smith-predictor

5.1 Nyquist Stability Criterion

Like the Bode Plot, the *Nyquist Diagram* is an alternative representation of the frequency response of a system. The Nyquist diagram for a transfer function $G(s)$ can be constructed from $|G(jw)|$ and $\angle G(jw)$ for different values of w . The Nyquist diagram and the *Nyquist Stability Criterion* can be used to assess the stability and robustness of a closed-loop system. Unlike the Bode Plot representation, the open-loop transfer function G_{OL} need not be stable for a Nyquist representation. Figure 5.1 is an illustrative example showing the Nyquist Plot of an open-loop transfer function $G_{OL}(s) = \frac{1}{2s+1}$.

The Nyquist Stability Criterion is stated in [27] as follows :

Theorem 1. *Consider an open-loop transfer function $G_{OL}(s)$ that is proper and has no unstable pole-zero cancellations. Let N be the number of times that the Nyquist plot for $G_{OL}(s)$ encircles the $(-1, 0)$ point in the clockwise direction. Also let P denote the number of poles of $G_{OL}(s)$ that lie to the right of the imaginary axis. Then, $Z = N + P$ where Z*

is the number of roots (or zeros) of the characteristic equation that lie to the right of the imaginary axis. The closed-loop system is stable if and only if $Z = 0$.

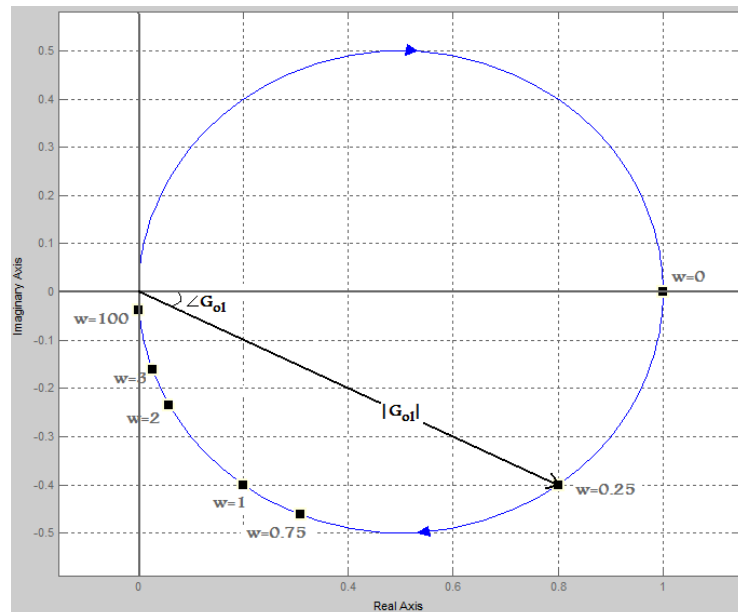


Fig. 5.1 The Nyquist diagram for $G_{OL}(s) = \frac{1}{2s+1}$ with $\mathcal{Re}(G(jw))$ on the x-axis and $\mathcal{Im}(G(jw))$ on the y-axis.

5.2 Smith-Predictor - The Theory

PID is an acronym for *Proportional*, *Integral* and *Derivative*, describing a type of controllers that take corrective action on the present, future, and past values of the error between the actual output of the system and the desired set-point.

The PID controller was first placed on the market in 1939 by Albert Callender and Allan Stevenson of Imperial Chemical Limited of Northwich and has remained the most widely used controller in process control until today. PID control theory, is a well known one in the control area, famous for its simplicity as well as the excellent control performance and robustness.

Whoever worked with a PID controller knows that a large deadtime in the system makes it harder to achieve simultaneous stability and performance. To see why it is the case, let us examine the following example.

Consider a closed-loop system comprising of a *Proportional* controller K with transfer function $K(s) = \mathcal{K}$, a plant with transfer function $\frac{1}{\tau s + 1}$ and let the sensor with unity transfer function add a deadtime of $e^{-\phi s}$. The open-loop transfer function of the system thus becomes:

$$G_{OL}(s) = \frac{\mathcal{K}e^{-\phi s}}{\tau s + 1}$$

Let us choose arbitrarily $\tau = 2$ and $\phi = 3$. The open-loop system has a stable pole at $s = -0.5$, thus to achieve closed-loop stability, the Nyquist diagram of $G_{OL}(s)$ should not encircle the point $(-1,0)$. The immediate effect of having a deadtime in G_{OL} is having the same deadtime appearing in the denominator of the transfer function of the closed-loop system. Then, As apparent from Figure 5.2 there will be a critical controller gain \mathcal{K}_c that cannot be exceeded. Any value of $\mathcal{K} > \mathcal{K}_c$ will render the closed-loop system unstable.

Thus, to maintain stability when deadtime is added to the system, the controller's gain has to be reduced. The reduction in the gain of the controller has an undesirable effect of deteriorating the system's performance.

Consequently, a Smith-Predictor was the industry's answer to those types of plants due to its effective deadtime compensation capabilities. Consider the feedback system in Figure 5.3, let K designate the controller, P the studied plant and T_d the deadtime rising from the sensors with corresponding transfer functions $K(s)$, $P(s)$ and $T_d(s)$. Thus the transfer

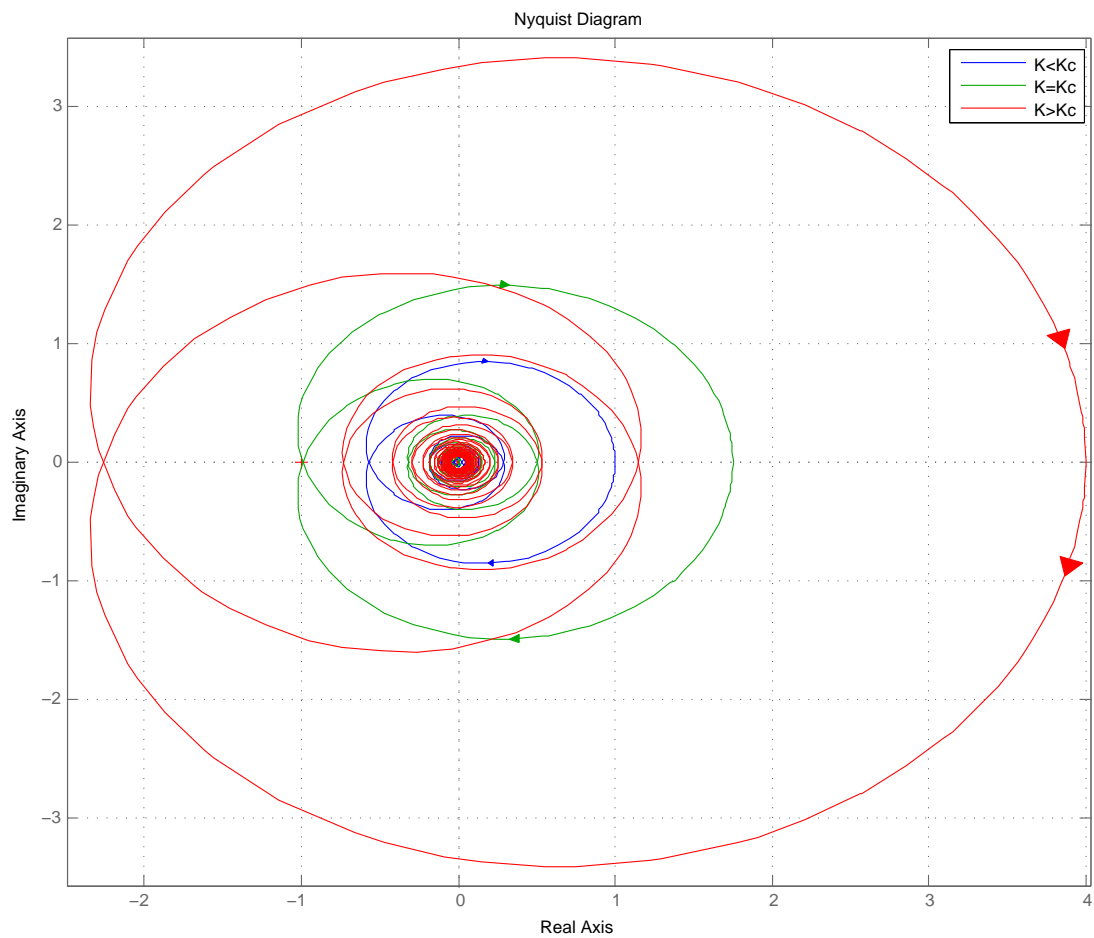


Fig. 5.2 The Nyquist diagram of the open-loop transfer function $G_{OL}(s) = \frac{K e^{-\phi s}}{\tau s + 1}$ for different values of K . K_c designates the critical controller gain that render the closed-loop system unstable.

function of the closed-loop system is:

$$T_{cl}(s) = \frac{Y(s)}{S(s)} = \frac{K(s)P(s)T_d(s)}{1 + K(s)P(s)T_d(s)}$$

As explained above, the deadtime $T_d(s)$ is now present in the denominator of $T_{cl}(s)$. The aim of the Smith-Predictor is then try to eliminate this unwanted appearance.

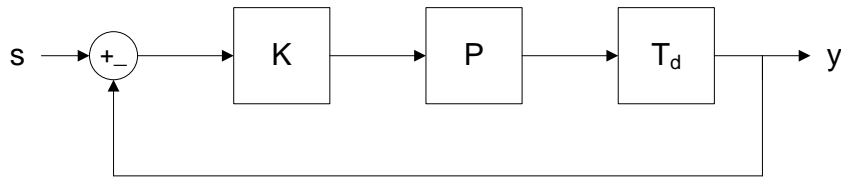


Fig. 5.3 A closed-loop system comprising of a controller, a plant and a deadtime with respective transfer functions $K(s)$, $P(s)$ and $T_d(s)$.

To improve the design, let P_m represents the model of the systems dynamics, T_{dm} , represents the model of the time delay, and e represents the error between the output of the model and the output of the plant. Thus, as shown in Figure 5.4 the model can be then split into the delayed system and the delay-free one.

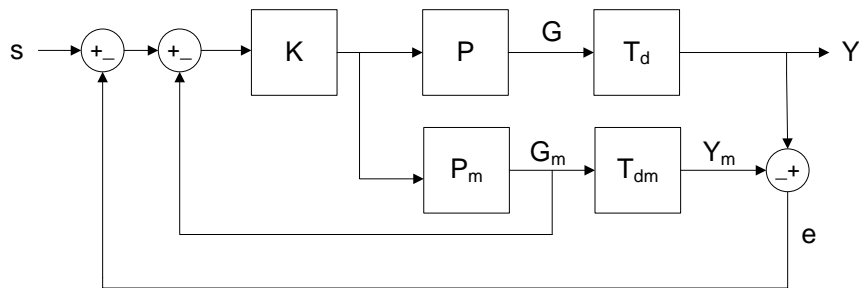


Fig. 5.4 The smith-predictor as an improved configuration for dead-time compensation purposes.

G is an unavailable fictitious variable, thus G_m is used for the feedback. In this setup, the controller would act on the modeled delay-free system P_m and regain the lost stability

margin. This layout can stabilize the nominal system but does not take into account model inaccuracies and external disturbances. To correct for these errors, signal "e" is then used in a cascade configuration closing a second feedback loop around the system. The controller K can be a PID, a PD (*Proportional, Derivative*) or PI (*Proportional, Integral*) controller. Depending on the desired control objectives, K can be tuned to be an aggressive or a smooth controller for either disturbance rejection or set-point tracking purposes.

In the ideal case where $P(s) = P_m(s)$ and $T_d(s) = T_{dm}(s)$ the closed-loop transfer function becomes:

$$\frac{Y(s)}{S(s)} = \frac{K(s)P(s)T_d(s)}{1 + K(s)P(s)}$$

As one can see the dead time is no longer present in the denominator and no loss in the stability margin of the system has occurred. A more conventional configuration of the Smith-Predictor Controller K_{smith} is shown in Figure 5.5, which is equivalent to the one shown in Figure 5.4.

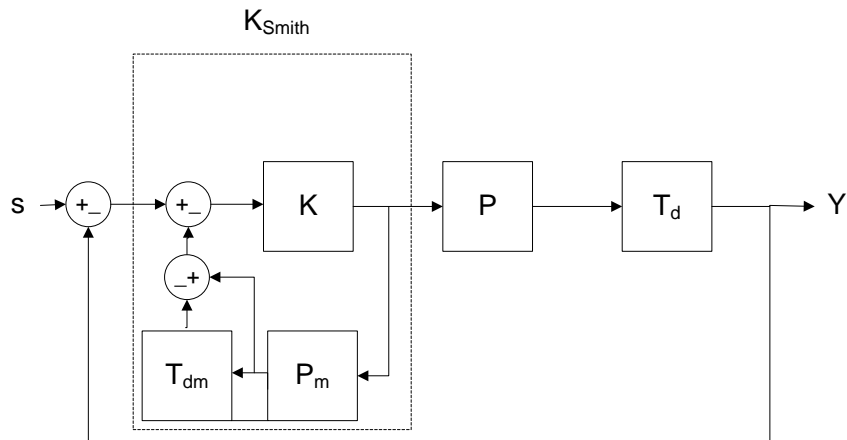


Fig. 5.5 The conventional smith-predictor configuration.

5.3 Smith-predictor - Design and Simulations

Approximating the deadtime added by the OSMP sensor as 30 minutes, and utilizing the non-linear system of the body's osmo-regulation derived above, a closed-loop system to control the OSMP in patients with CDI was conceived. Figure 5.6 shows the Matlab's *simulink* model.

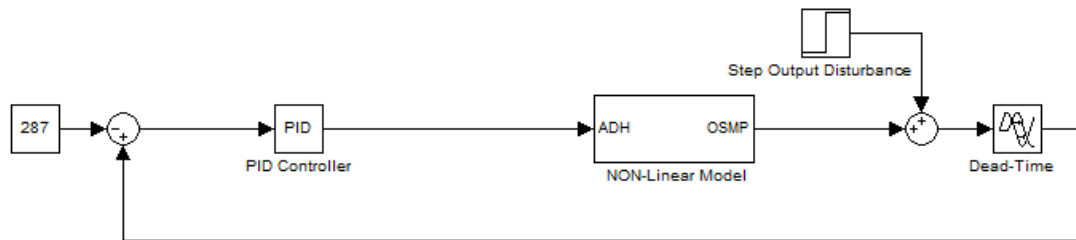


Fig. 5.6 Simulink model of the closed-loop osmo-regulatory system utilizing a PD controller.

A PD controller established desired closed-loop performance results. Where, in this case performance was defined as the time that it takes the system to return to its nominal condition (OSMP level of 287 mOsm/l) after an output step disturbance of 20 mOsm/l. Setting the controller's derivative action gain k_d to 0.7 and varying the controller's proportional action gain k_p from 0.05 to 0.1 and 0.3 we obtained the responses shown in Figure 5.7.

To be noted that an output step disturbance was chosen over any other kind of disturbances due to the fact that it models a persistent and sudden change in the plasma osmolality level of an individual, putting significant pressure on the controller. The causes of such a disturbance could be due to finite energy input disturbances such as an intermittent water loading of an individual [34], water deprivation [35], intermittent hypertonic or hypotonic solution injection [36], etc...

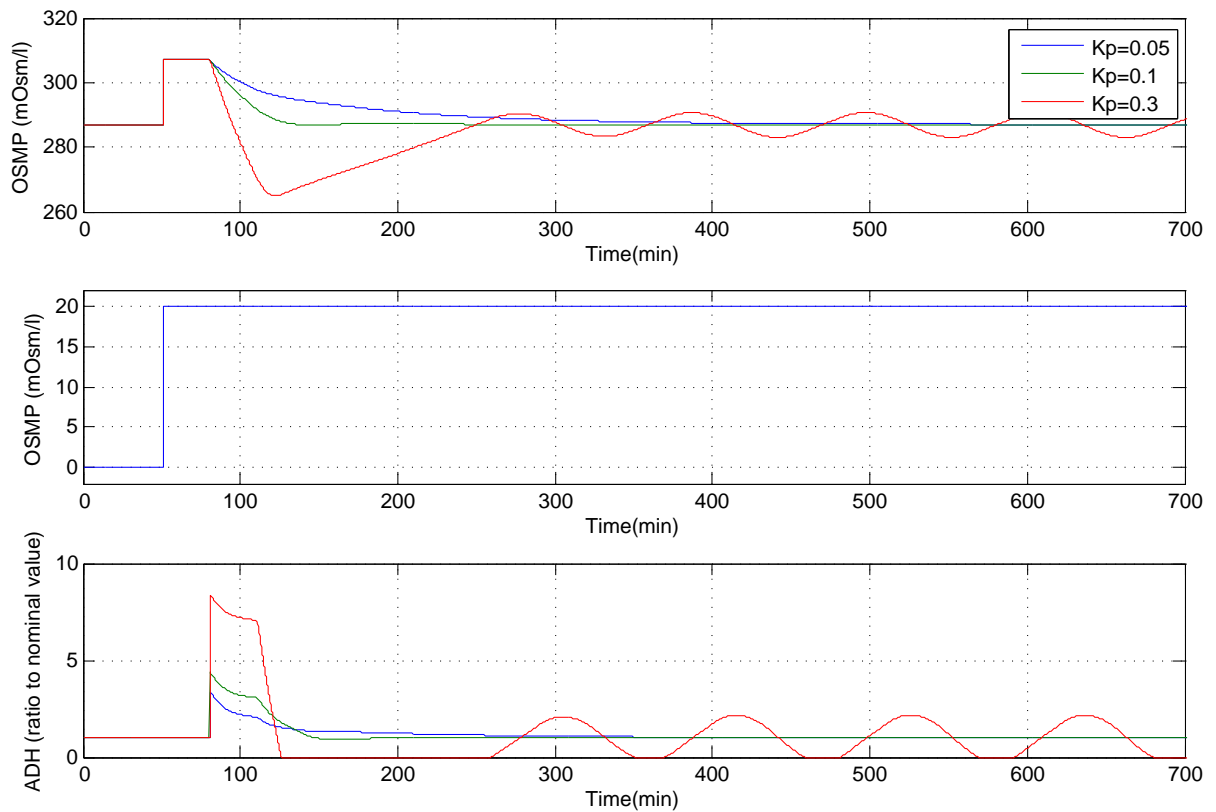


Fig. 5.7 The response of the osmo-regulatory closed-loop system to an output step disturbance of 20 mOsm/l. The Controller used is a PD controller with fixed derivative gain of 0.7 and a varying proportional gain k_p . The output of the controller is also shown for each case.

At a value of $\mathcal{K}_c = k_p = 0.3$ the systems response is oscillatory. Consequently, with k_d being at 0.7 and to maintain stability, the proportional action gain has to be kept below the critical gain \mathcal{K}_c at all times.

Therefore, to achieve a higher performance, a PD (*Proportional, Derivative*) controller in a smith predictor configuration was then employed to compensate for the deadtime added by the sensors (Figure 5.8).

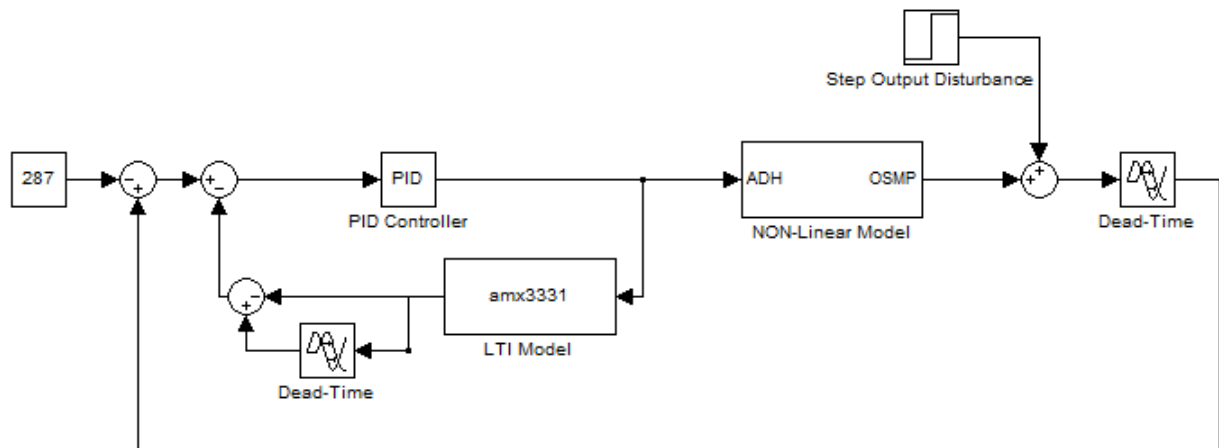


Fig. 5.8 Simulink model of the closed-loop osmoregulatory system utilizing a PD controller in a smith-predictor configuration.

Using the same derivative gain $k_d = 0.7$ as before and varying the proportional gain of the PD controller from 0.05 to 0.1 and 0.3 we obtained the responses shown in Figure 5.9. Clearly the system has now a higher stability margin, at $k_p = 0.3$ the system still performs well.

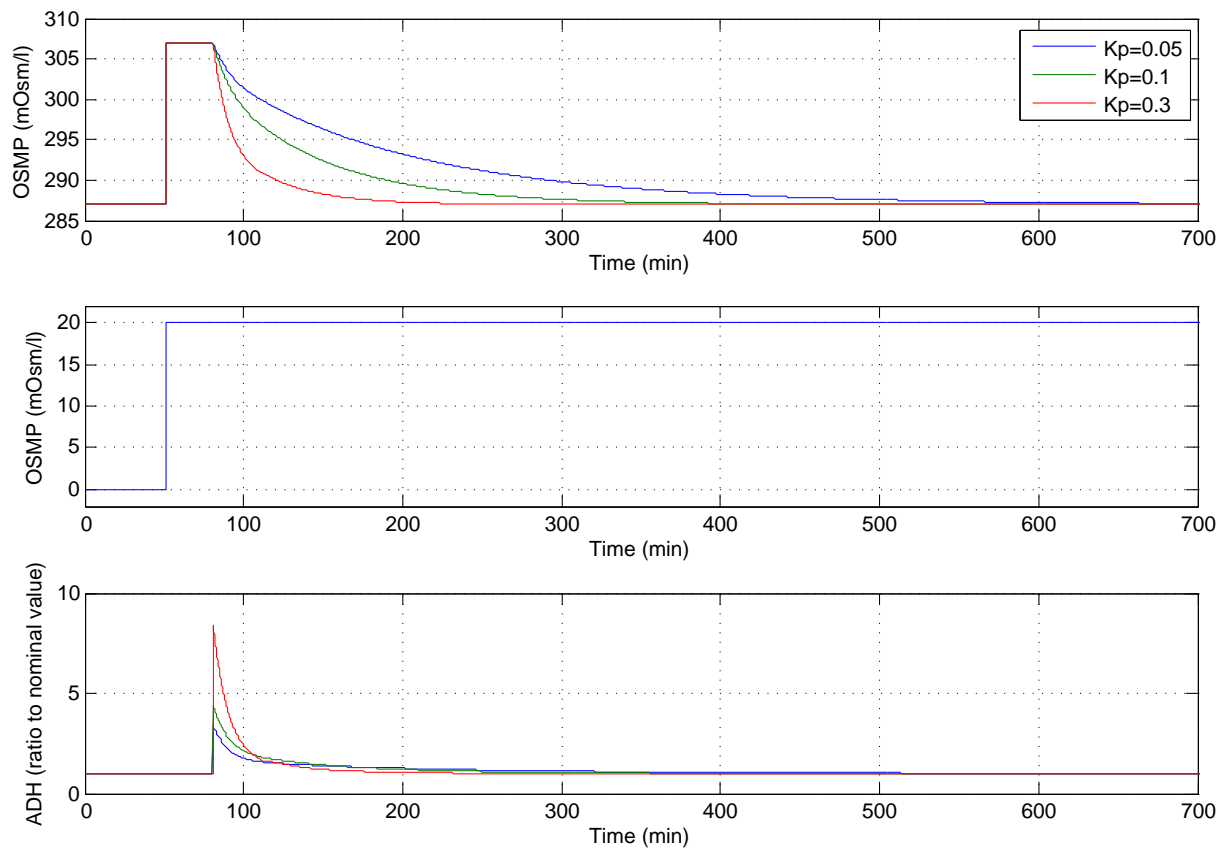


Fig. 5.9 The response of the osmo-regulatory closed-loop system to an output step disturbance of 20 mOsm/l. The Controller used is a PD controller in a smith-predictor configuration, with fixed derivative gain of 0.7 and a varying proportional gain k_p . The output of the controller is also shown for each case.

One disadvantage of the Smith-Predictor approach is that it is model-based; that is, a fairly accurate model of the studied system is required [27]. If model inaccuracies or uncertainties are present in the system (due to the fact that each individual renal system is somehow unique), the predictive model will be inaccurate and the controller performance will deteriorate, sometimes to the point of having closed-loop instability.

Another issue that arises with the PID/Smith predictor controller that would be problematic in a biomedical system, is the uncontrollable bound of the controller's output. In this type of control no automatic adjustment of the controller's output is possible. Therefore to limit the ADH concentration in the blood stream, a saturation block has to be installed on the controller's output, keeping ADH concentration within a certain healthy range. Unfortunately, this option greatly degrades the control system's performance. In the following chapter, we will see how this issue can be easily resolved with \mathcal{H}_∞ Optimal Control.

Chapter 6

\mathcal{H}_∞ Optimal Control

6.1 \mathcal{H}_∞ - The Theory

Before we start our discussion on H-infinity (\mathcal{H}_∞) optimal control theory let us briefly introduce some basic concepts regarding the p-norm; Specifically the 2-norm of a signal and the ∞ -norm of a system.

Uniformly speaking, the ∞ -norm -sometimes referred to as the \mathcal{H}_∞ norm- is the measure of how big the frequency response of a system is. Let $P(s) \in \mathbb{R}^{m \times n}$ be a real rational transfer function matrix. If $P(s)$ is stable and proper then

$$\|P(s)\|_\infty = \max_{w \in \mathbb{R}} \bar{\sigma}(P(jw))$$

where, $\bar{\sigma}$ denotes the maximum singular value.

In time domain the same norm can be interpreted as the maximum *rms* energy gain of

the system over all bounded inputs.

$$\|P(s)\|_\infty = \sup_{u(t) \neq 0} \frac{\|y\|_2}{\|u\|_2}$$

where $y(s) = P(s)u(s)$, and $y(s)$ and $u(s)$ are the *Laplace Transforms* of $y(t)$ and $u(t)$ respectively. \sup denotes the supremum (or the least upper bound) and $\|\cdot\|_2$ denotes the 2-norm defined in time domain as:

$$\|x(t)\|_2 = \sqrt{\int_{-\infty}^{\infty} |x(t)|^2 dt}$$

In this work, the \mathcal{H}_∞ -norm was chosen as an optimization criterion over that of the \mathcal{H}_2 -norm due to the fact that it introduces a more severe constraint. \mathcal{H}_2 optimal control focuses on the optimization of the average behavior of the system to white noise; In contrast, \mathcal{H}_∞ optimal control deals with minimizing the maximum input to output gain of the system.

Thus, \mathcal{H}_∞ optimal control theory addresses the issue of designing a stabilizing controller that minimizes the peak value of some desired closed-loop frequency response functions within a control system. To clarify this, consider by way of example the SISO feedback system of Figure 6.1, where P and K designate the plant's and controller's transfer function respectively. The signal d_o represents a disturbance acting on the system and y is the control system output. It follows that $y = S_o d_o$, where

$$S_o = \frac{1}{I + PK}.$$

S_o is called the *sensitivity* of the feedback system. As the name implies, S_o characterizes how sensitive the control system's output is to an output disturbance. The objective of \mathcal{H}_∞ control would then ideally try to achieve $S = 0$.

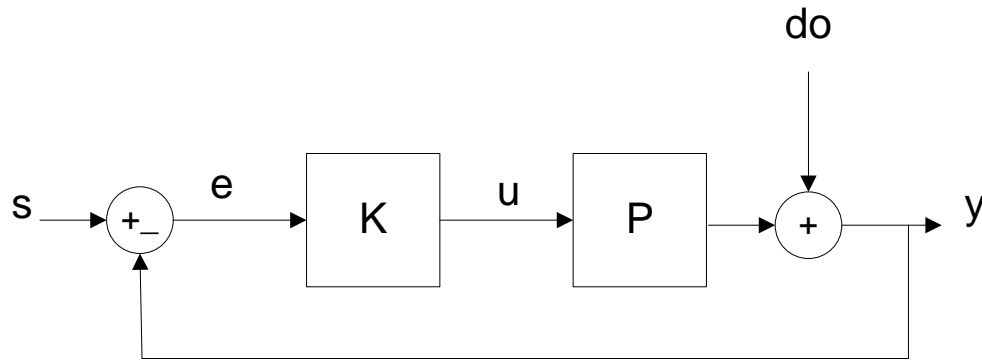


Fig. 6.1 A SISO feedback system where P and K designate the plant's and controller's transfer function. s and y designate the input and output of the system respectively. respectively

This problem was originally considered by George Zames who posed it as a mathematical optimization problem to find a stabilizing controller K that minimizes the maximum value of the sensitivity function. This maximum value is defined as

$$\|S_o\|_\infty = \sup_{w \in \mathbb{R}} |S_o(jw)|.$$

The supremum is used since the maximum of certain functions may not be attainable by a finite frequency. The reason behind this problem setup is that if the peak value ($\|S_o\|_\infty$) of the sensitivity function is below a certain small $\gamma \in \mathbb{R}$, then

$$|S_o| < \gamma, \forall w.$$

The disturbances are therefore uniformly attenuated over all frequencies.

Now suppose that the disturbance d_o has a finite energy defined as:

$$\mathcal{E} = \|d_o\|_2^2 = \int_{-\infty}^{+\infty} |d_o|^2 dt$$

then,

$$\|S_o\|_\infty = \sup_{\|d_o\|_2 < \infty} \frac{\|y\|_2}{\|d_o\|_2}$$

The minimization of $\|S_o\|_\infty$ is denoted by worst-case optimization [37], because it tries to minimize the effect of the worst disturbance (a harmonic disturbance at w_p), where w_p denotes the frequency where $|S_o| = \|S_o\|_\infty$.

Unfortunately, the frequency response of any physical plant and controller will roll off at high frequencies. Then,

$$P(jw)K(jw) \xrightarrow{w \rightarrow \infty} 0 \text{ and } S_o \xrightarrow{w \rightarrow \infty} 1.$$

For performance purposes, low frequencies are in general the frequencies of interest and how small S_o is at those frequencies is not reflected in $\|S_o\|_\infty$. Therefore, just minimizing $\|S_o\|_\infty$ is not very useful. Consequently, a frequency dependent weighting function W is introduced and the weighted *sensitivity* is then minimized:

$$\|WS_o\|_\infty = \sup_{w \in \mathbb{R}} |W(jw)S_o(jw)|$$

The weighting functions are a useful addition to the theory as they are used to reflect different minimization objectives at different frequencies.

Different weighting functions could also be added at different locations to achieve differ-

ent control objectives. Consider Figure 6.2, W_d is used to describe the frequency content of the expected output disturbance, W_e defines the performance objectives by putting more weight on the frequencies of interest, W_u is used to shape and limit the control signal u .

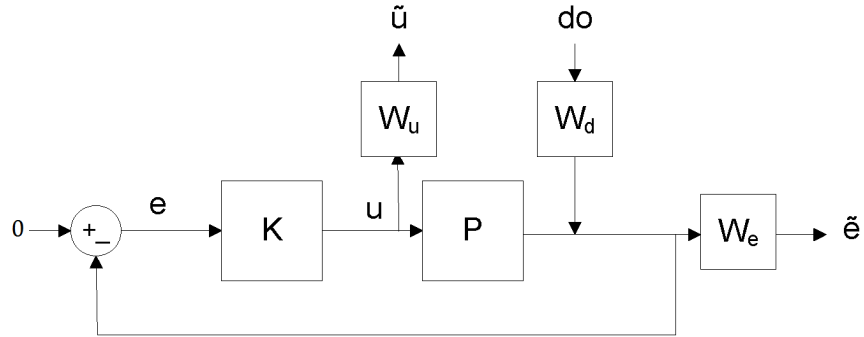


Fig. 6.2 A SISO feedback system showing different weighting functions added at different locations to achieve different control objectives.

Here, the \mathcal{H}_∞ performance is achieved if under worst possible disturbance:

$$\|W_e S_o W_d\|_\infty = \sup_{\|d_o\|_2 < \infty} \frac{\|\tilde{e}\|_2}{\|d_o\|_2} = \sup_{\|d_o\|_2 \leq 1} \|\tilde{e}\|_2$$

$$\|W_u K S_o W_d\|_\infty = \sup_{\|d_o\|_2 < \infty} \frac{\|\tilde{u}\|_2}{\|d_o\|_2} = \sup_{\|d_o\|_2 \leq 1} \|\tilde{u}\|_2$$

In order to utilize \mathcal{H}_∞ control theory, the system has to be represented according to the standard configuration shown in Figure 6.3.

where,

$$P(s) = \left[\begin{array}{c|cc} A & B_1 & B_2 \\ \hline C_1 & 0 & D_{12} \\ C_2 & D_{21} & 0 \end{array} \right]$$

With the assumptions that:

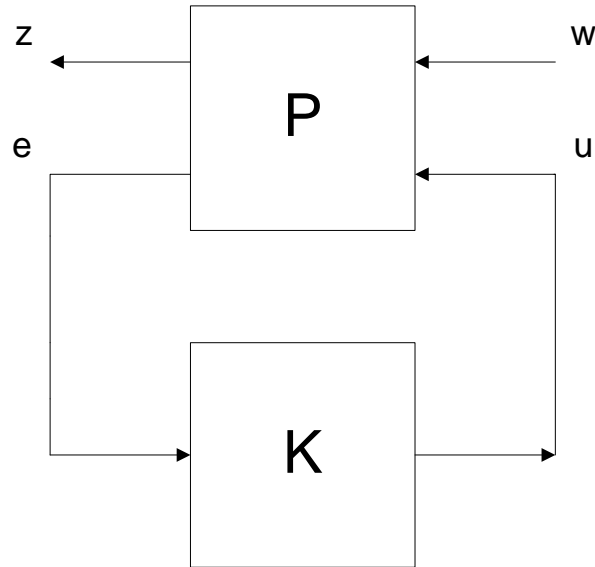


Fig. 6.3 Standard system configuration for an H-infinity problem.

- (A, B_1) is controllable and (C_1, A) is observable.
- (A, B_2) is stabilizable and (C_2, A) is detectable.
- $D_{12} [C_1, D_{12}] = [0 \ I]$
- $\begin{bmatrix} B_1 \\ D_{21} \end{bmatrix} D_{21}^* = \begin{bmatrix} 0 \\ I \end{bmatrix}$

Plant P has two inputs, the exogenous input w , that includes the reference signal and disturbances, and the control signal u (i.e. the manipulated variable). P has also two outputs, the error signals e and the measured variables z .

Through mathematical manipulations, it is possible to express z as:

$$z = F_\ell(\mathbf{P}, \mathbf{K}) w$$

Where the F_ℓ , known as the lower linear fractional transformation is defined as:

$$F_\ell(\mathbf{P}, \mathbf{K}) = P_{11} + P_{12} \mathbf{K} (I - P_{22} \mathbf{K})^{-1} P_{21}$$

The objective of \mathcal{H}_∞ control is to find a controller \mathbf{K} such that $F_\ell(\mathbf{P}, \mathbf{K})$ is minimized according to the \mathcal{H}_∞ norm, where:

$$\|F_\ell(\mathbf{P}, \mathbf{K})\|_\infty = \sup_{\omega} \bar{\sigma}(F_\ell(\mathbf{P}, \mathbf{K})(j\omega)) = \gamma \quad (6.1)$$

Referring to Figure 6.4 below:

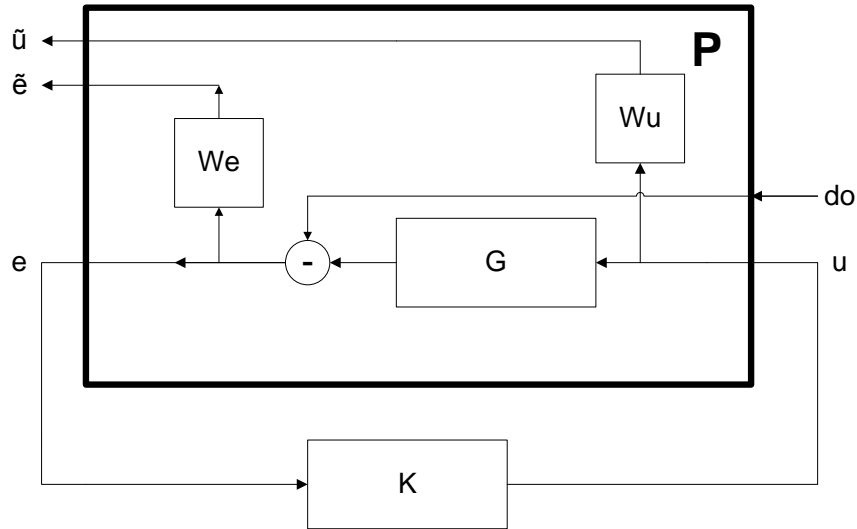


Fig. 6.4 The augmented plant P , showing the internal configuration and weighting functions.

Then,

- $\tilde{e} = eW_e = (T_{do\tilde{e}})do$
- $\tilde{u} = uW_u = (T_{do\tilde{u}})do$

Let, $z = \begin{bmatrix} \tilde{e} \\ \tilde{u} \end{bmatrix}$ and $w = do$. by trying to achieve a $\gamma < 1$ we can guarantee that:

$$\|T_{doz}\|_\infty < 1$$

and,

$$\|T_{do\tilde{e}}\|_\infty < 1$$

$$\|T_{do\tilde{u}}\|_\infty < 1$$

And consequently,

$$|T_{doe}(j\omega)| < |W_e^{-1}(j\omega)|, \quad \forall \omega$$

$$|T_{doe}(j\omega)| < |W_u^{-1}(j\omega)|, \quad \forall \omega$$

6.2 \mathcal{H}_∞ - Design and Simulations

By choosing the weighting functions carefully we could limit the amount of ADH in the system while achieving desired performance criteria.

The weighting functions were chosen as follows:

$$W_e = 500 \frac{\frac{1}{10^{-1.5}}s + 1}{\frac{1}{10^{-4.6}} + 1}$$

$$W_u = 10$$

The ADH level in the body and consequently the control input of the plant cannot go unbounded and has to be maintained below a certain limit. This constraint does not change as a function of frequency, hence the input weight is set to $Wu = 10, \forall w$. Performance weight selection is based on engineering judgment and the need to satisfy $|S_o| < \frac{1}{|W_e|} \forall w$. W_e (Figure 6.5) was designed to have a high gain a low frequencies, and a disturbance rejection of at least 500:1 at DC then rolls off around $w = 10^{-4}$ rad/s, thus maintaining a good performance at frequencies of interest. Note that the time delay was not included in the model of the system, and was added later for simulation and system testing purposes.

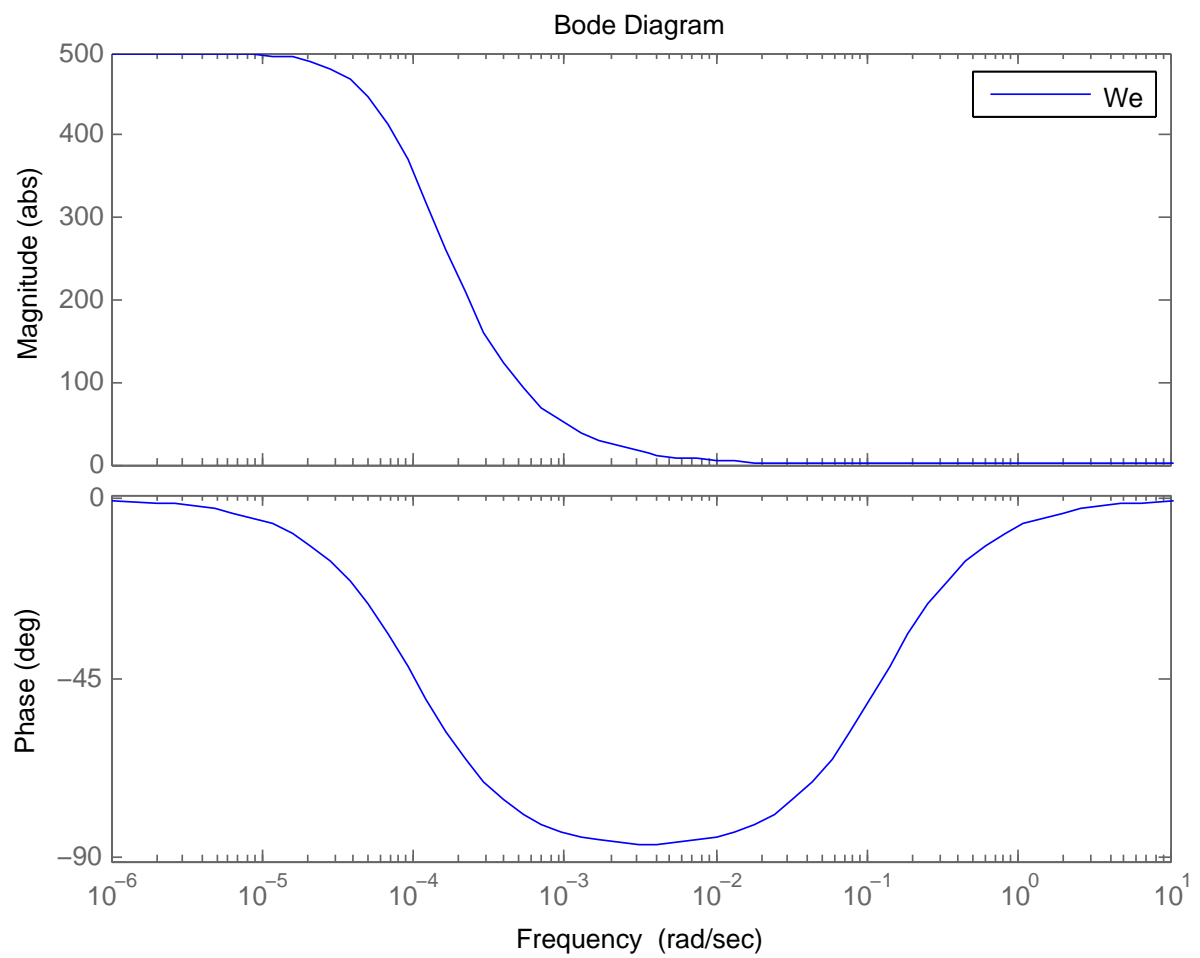


Fig. 6.5 The performance objectives defined by the weighting function W_e .

Using the Hinfyn command located in Matlab's Robust Control toolbox and with the above described system configuration, a γ of 0.8087 was achieved with the following \mathcal{H}_∞ optimal controller K :

$$K(s) = \frac{-0.1838s^3 - 0.01211s^2 - 0.001122s - 6.599 \times 10^{-8}}{s^4 + 2.695s^3 + 0.1774s^2 + 0.01596s + 4.007 \times 10^{-7}}$$

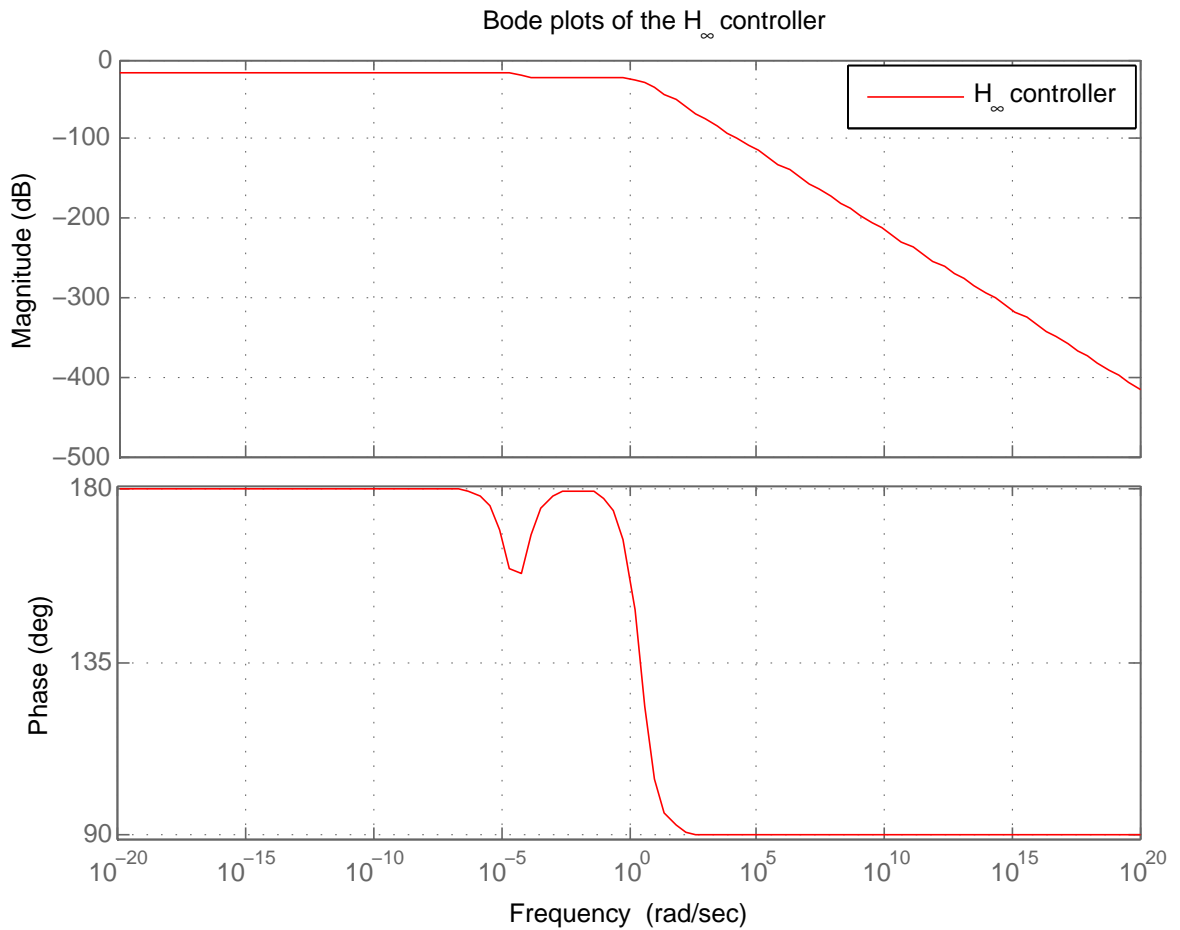


Fig. 6.6 The bode plot of the \mathcal{H}_∞ optimal controller.

Figure 6.7 shows the response of the closed-loop system after an output step disturbance of 20 mOsm/l. As expected the variation in the controller's output Δu is limited with respect to the controller's response.

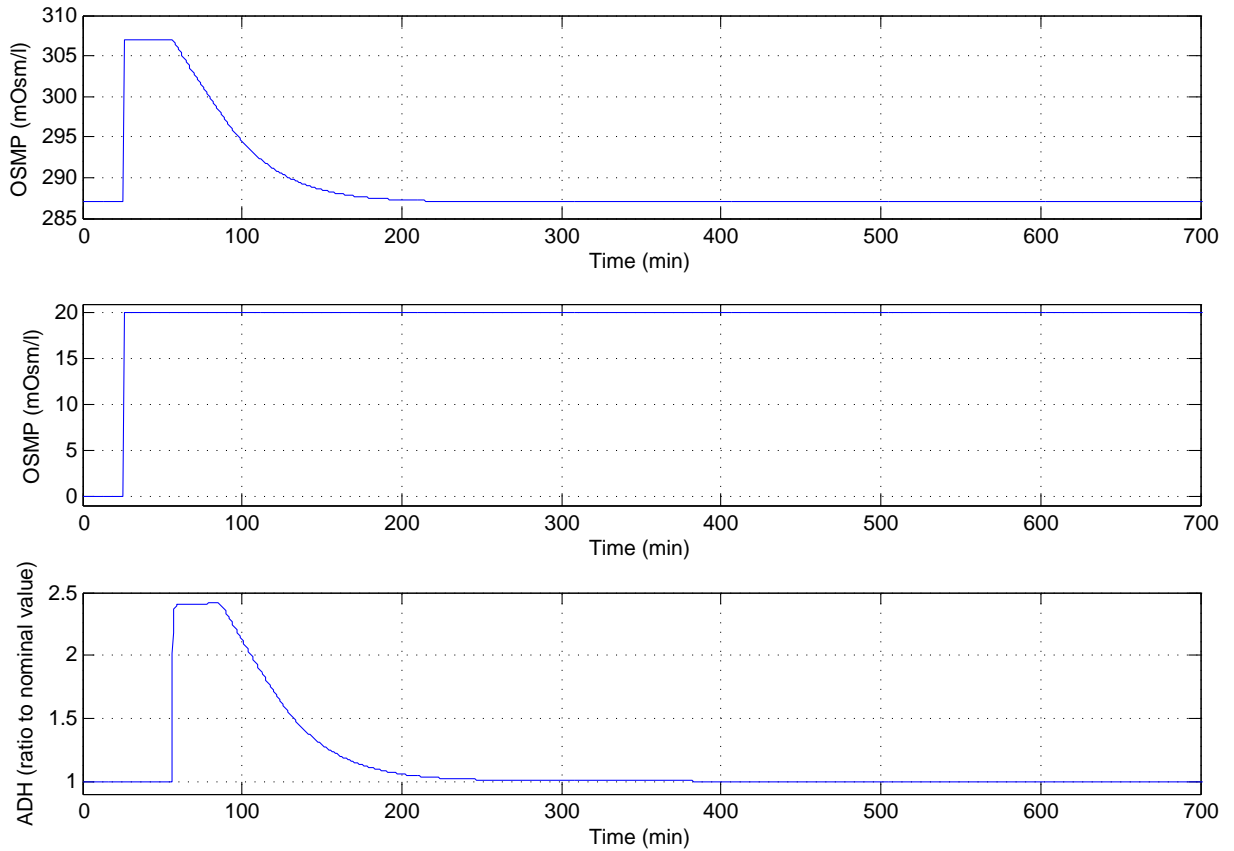


Fig. 6.7 The response of the Omsoregulatory closed-loop system to an output step disturbance of 20 mOsm/l. The controller used is the \mathcal{H}_∞ optimal controller K . Lastly, the output of the controller is shown.

Chapter 7

Robust Control

For the abundance of theory and ease of study of Linear Time Invariant (LTI) systems in the Systems and Control academic and non-academic community; any control systems engineer trying to describe a physical system would thrive to acquire an LTI model for it. Unfortunately, LTI models usually describe the actual system's dynamics only approximately. *Model uncertainties* can have several different sources. In general, physical processes are non-linear, if the LTI model is obtained via linearization, then the model is only accurate around the operating point. In other cases, some systems can have parameters that are uncertain, they can vary within a specific range depending on external factors and no one model can accurately describe the behavior of the system in each one of those instances. Whether it is modeling errors, neglected non-linearities or parametric uncertainties, they can all be accounted for using many different strategies. In the following, we will be designing a control system that is *robust*, i.e. a control system that will be stable and achieve a certain degree of performance in the presence of unavoidable uncertainties in the system. Consequently, we will not be dealing with a single LTI system model $G(s)$ but with a perturbed one $G_p(s)$ comprising of a family of LTI models.

7.1 Uncertainty Modeling and Robust Control Theory

7.1.1 Unstructured Uncertainty and The Small Gain Theorem

In many instances, modeling uncertainties corresponding to different parts of the system can be lumped or combined into one single perturbation block Δ . Depending on the system, the uncertainty block dynamics can be described in many different ways. Suppose that the perturbed plant $G_p(s)$ and the nominal plant $G(s)$ are related as follows:

$$G_p(jw) = G(jw) + \Delta_a, \|\Delta_a\| < \delta_a, \forall w$$

where, δ_a is the maximum singular value (bound) of Δ_a at all frequencies. This form of representation is called additive uncertainty representation since the uncertainty is added to the nominal model. Then the robust control theory assumes that the unknown "true" model belongs to the set of plants $G_p(s)$. Figure 7.1 is a system representation of the additive uncertainty.

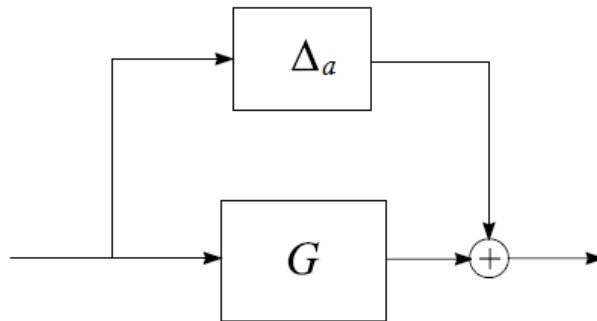


Fig. 7.1 The additive uncertainty system configuration.

Other ways to represent uncertainties are also available, such as the:

- Output multiplicative uncertainty $G_p(jw) = (\mathbf{I}_p + \Delta_m(jw))G(jw)$ with $\|\Delta_m\| < \delta_m, \forall w$

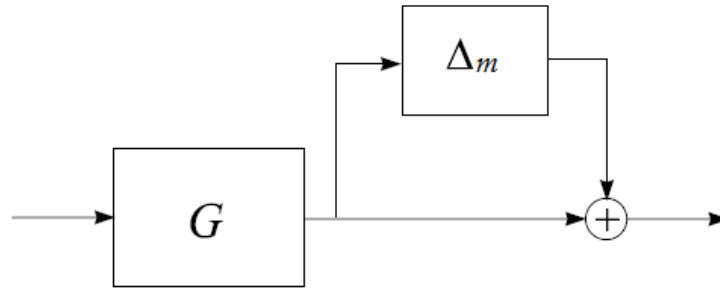


Fig. 7.2 The output multiplicative uncertainty system configuration.

- Input multiplicative uncertainty $G_p(jw) = G(jw)(\mathbf{I}_m + \Delta_m(jw))$ with $\|\Delta_m\| < \delta_m, \forall w$

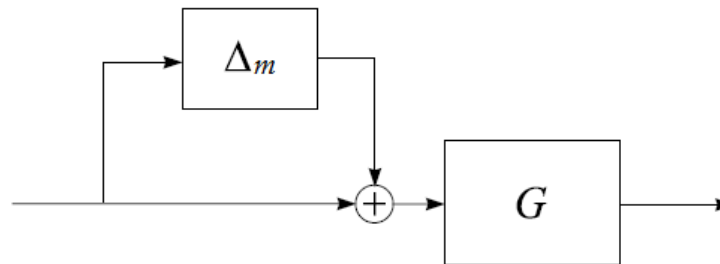


Fig. 7.3 The input multiplicative uncertainty system configuration.

Whatever the chosen uncertainty representation, the feedback control system can have an LFT representation as shown in Figure 7.4.

Given a model of this form, it is then easy to rearrange the system into the form shown in Figure 7.5 where $M = F_\ell(\mathbf{P}, \mathbf{K})$, then:

$$e = F_u(\mathbf{M}, \Delta)u = (\mathbf{M}_{22} + \mathbf{M}_{21}\Delta(\mathbf{I} - \mathbf{M}_{11}\Delta)^{-1}\mathbf{M}_{12})u$$

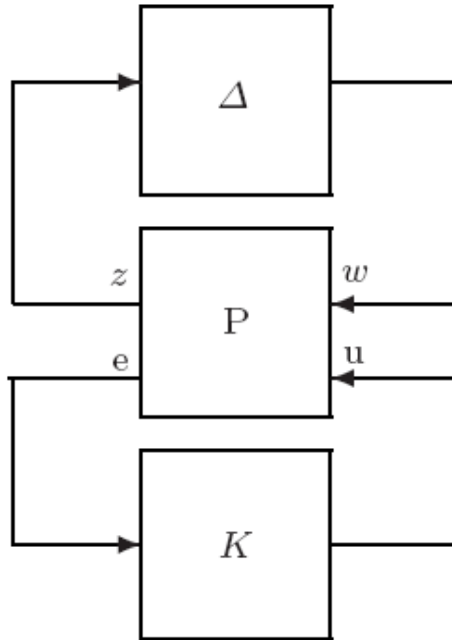


Fig. 7.4 The standard LFT configuration.

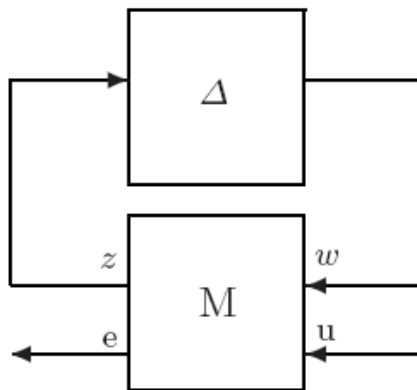


Fig. 7.5 The standard M- Δ configuration.

The *small gain theorem* (Zames, Sandberg) states that under the assumption that:

- $\mathbf{M}(s) \in \mathcal{R}\{\mathcal{H}_\infty\}$
- $\Delta(s) \in \mathcal{R}\{\mathcal{H}_\infty\}$

The $\mathbf{M}-\Delta$ feedback interconnection shown in Figure 7.5 is stable for every perturbation $\Delta(s)$ such that $\|\Delta\|_\infty < 1$ *if and only if* $\|\mathbf{M}\|_\infty \leq 1$.

Clearly $\|\Delta\|_\infty < 1$ is at first glance a condition that would appear too restrictive to the theory, but in fact could be accounted for by rewriting the perturbation block as

$$\Delta(s) = \tilde{\Delta}(s)W(s)$$

where $\tilde{\Delta}(s)$ is the unit norm perturbation set; $\bar{\sigma}(\Delta(jw)) \leq \bar{\sigma}(W(jw))$ and then incorporating $W(jw)$ inside the M block.

7.1.2 Structured Uncertainty and The Structured Singular Value

As previously discussed, the uncertainty in the model can come from different sources. One way to account for those uncertainties is to try to bound all the possible perturbation in the nominal plant with a single *full* complex block. This unstructured uncertainty representation may generate a much larger set of perturbed plant that will render this approach too conservative. Another approach is to model each source of uncertainty separately. In this case the perturbation block Δ will have a diagonal or block diagonal structure. Let,

$$\Delta_s = \text{diag}(\Delta_1(jw), \Delta_2(jw), \dots, \Delta_n(jw)), \bar{\sigma}(\Delta_i) < \delta.$$

where δ defines an upper bound on the size of the maximum singular value of any uncertainty block Δ_i . To further elaborate on the concept, consider the question: What is the

maximum value of δ for which the closed-loop system will remain stable? As in the unstructured uncertainty case, we can still apply the *small gain theorem* to the above problem, but the result will be conservative, since the structure of the matrix Δ will not be taken into account. The SGT will not take into account that most of the entries of Δ are in fact zero. Thus, the SGT will consider a larger set of uncertainty than is in fact possible, and the resulting robustness measure will be too conservative. In order to get a non-conservative solution, Doyle [4, 5], introduced the structured singular value μ_{Δ_s} :

$$\mu_{\Delta_s}(\mathbf{M}) = [\min \|\Delta_s\| : \det(\mathbf{I} - \mathbf{M}\Delta_s) = 0]^{-1}$$

The derivation of the robust stability theorem for structured perturbation (small - μ theorem) is quite complex, so let us skip directly to the results.

The Small- μ Theorem is stated as follows :

Theorem 2. *Assume controller $K(s)$ is stabilizing for the nominal plant $P(s)$. Then given $\beta > 0$, the closed-loop system in Figure 7.4 is well-posed and internally stable for all $\|\Delta_s\|_\infty < \beta$ if and only if:*

$$\sup_{w \in \mathcal{R}} \mu_{\Delta_s} \{F_\ell[\mathbf{P}(jw), \mathbf{K}(jw)]\} \leq \frac{1}{\beta}$$

Then, if the structured perturbation is normalized, i.e. $\|\tilde{\Delta}_s\|_\infty < 1$, the condition becomes:

$$\sup_{w \in \mathcal{R}} \mu_{\Delta_s} \{F_\ell[\mathbf{P}(jw), \mathbf{K}(jw)]\} \leq 1$$

7.2 Robust Performance

One way of defining a performance specification is to require that the maximum singular value of the frequency response matrix from u to e lies below some weighting function $W_p(jw)$. To achieve robust performance these specification have to hold for any uncertainty $\Delta_i \in \Delta_s$. Let, Ω a new structured uncertainty:

$$\Omega = \text{diag}(\Delta_1(jw), \Delta_2(jw), \dots, \Delta_n(jw), \Delta_p(jw)), \bar{\sigma}(\Delta_i) < \delta.$$

where, Δ_p was added to account for the new performance objectives specifications. Then Robust performance is achieved *if and only if*

$$\sup_{w \in \mathcal{R}} \mu_{\Omega} \{F_{\ell}[\mathbf{P}(jw), \mathbf{K}(jw)]\} \leq 1$$

where Ω is normalized, i.e. $\|\Omega\|_{\infty} < 1$

7.3 Robust Control - Design and Simulation

At low frequencies, below 2 rad/s, we would like $G_p(s)$ to vary up to 25% from its nominal state. Around 1 rad/s the percentage variation starts to increase and reaches 250% at approximately 100 rad/s. These specifications can be taken into account with an output multiplicative uncertainty model where the percentage of model uncertainty is represented by:

$$\Delta_m(s) = \widetilde{\Delta}_m(s)W_m(s)$$

where the weight W_m is shown in Figure 7.6.

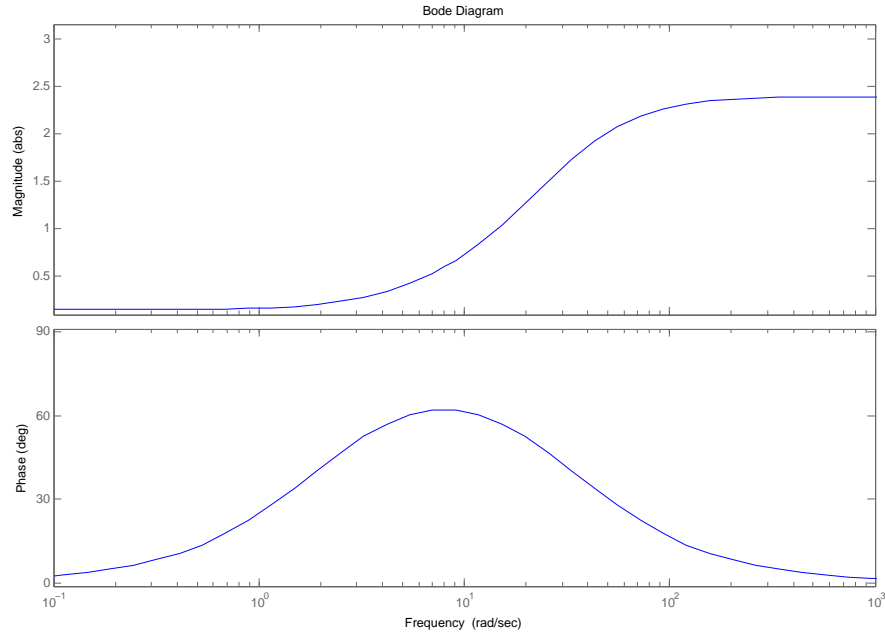


Fig. 7.6 The bode plot of the percentage of the multiplicative model uncertainty.

To add robustness to the control system, parametric uncertainty can also be added to $G_p(s)$. The nominal LTI Osmo-regulatory system as defined previously is:

$$G(s) = \frac{-0.2283s^2 - 0.01486s - 0.001346}{s^3 + 0.06588s^2 + 0.006106s + 3.591 \times 10^{-7}}$$

$G(s)$'s DC gain is defined as

$$G(s)_{DC} = |G(s)|_{s=0} = \frac{0.001346}{3.591 \times 10^{-7}}$$

The $G(s)_{DC}$ defines the sensitivity of the system as well. This sensitivity, as not to be confused with the sensitivity $S(j\omega)$ of the closed-loop system, characterizes the ability of the antidiuretic hormone (ADH) to affect the plasma osmolality (OSMP). As an example, if a nominal ADH value of 1 is needed to achieve a nominal OSMP value of 287 mOsm/l at a

certain sensitivity s_n ; If that sensitivity is increased to $s > s_n$, we would need a lower ADH value to achieve the same nominal value of the plasma osmolality. The sensitivity is a parameter that varies between individuals. By defining a family of LTI models $G_p(s)_{parametric}$ such that:

$$0.9 G(s)_{DC} < G_p(s)_{parametric_{DC}} < 1.1 G(s)_{DC}$$

and build a robust controller to $G_p(s)_{parametric}$, we would then have obtained a compensator that is robust to 10% change in the sensitivity of OMSP to ADH.

Let $G(s)$ be written in the following general format:

$$G(s) = \frac{a_2 s^2 + a_1 s + a_0}{b_3 s^3 + b_2 s^2 + b_1 s + b_0}$$

Then

$$G(s)_{DC} = \frac{a_0}{b_0}$$

Consequently, by varying a_0 by $\pm 10\%$ we can achieve a variation of 10% in the system's sensitivity. Using Matlab's "ureal" and "sample" tools in the *Robust Control Toolbox*, five samples of the parametric uncertainty are chosen randomly and a rectangular pulse at time $t = 400min$ is applied to the open-loop Osmoregulatory system whose block diagram is previously shown in Figure 4.1 (the block is repeated in Figure 7.7 for convenience). Figure 7.8 shows the open-loop response of the perturbed system $G_p(s)_{parametric}$.

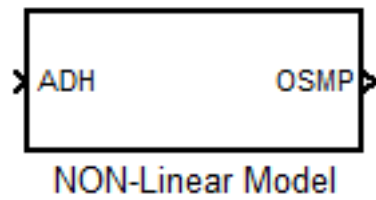


Fig. 7.7 The Simulink's nonlinear osmoregulatory system.

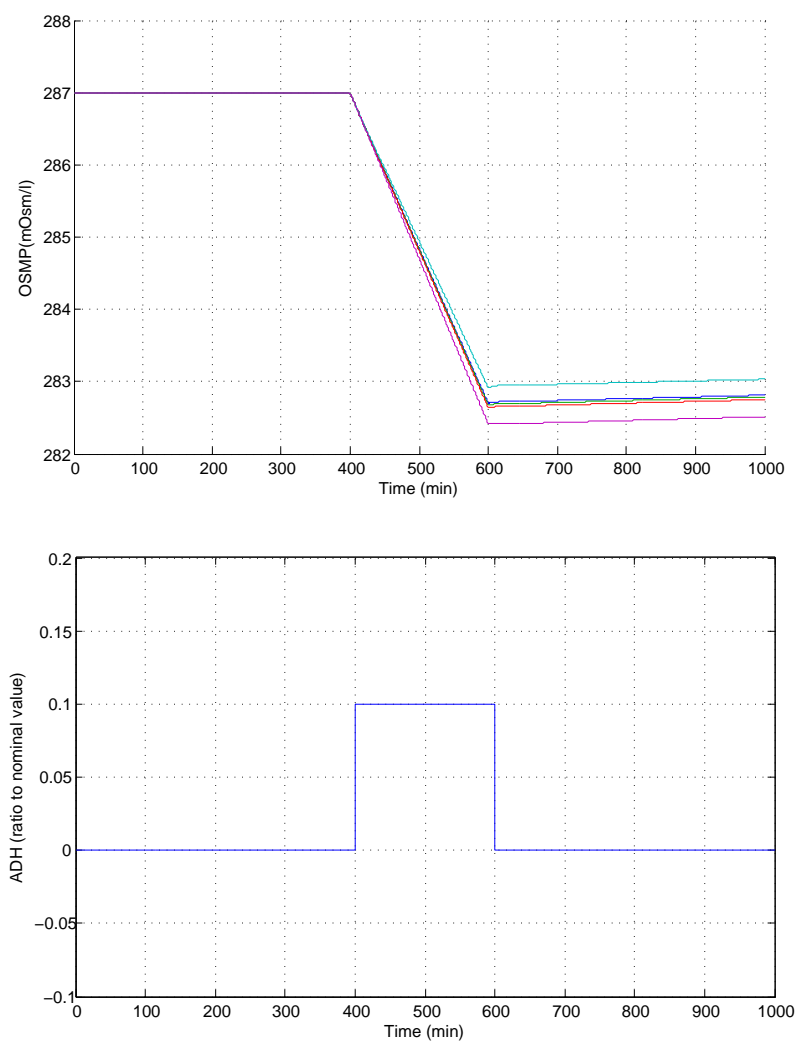


Fig. 7.8 Plots of the open-loop response of the perturbed system $G_{p(s)}_{parametric}$ (above) subject to a rectangular pulse at time $t = 400min$ (below).

We then built a perturbed system $G_p(s)$ comprising of the above described parametric uncertainty and output multiplicative uncertainty. Then, using *dksyn* tool in the *Robust Control Toolbox* we synthesized a robust controller K for the uncertain open-loop plant model $G_p(s)$ via the D-K algorithm (please refer to K.Zhou and J.Doyle's work on robust control [38]) for μ -synthesis. This compensator will achieve robust stability and robust performance of the control system *if and only if* the value of $\mu < 1$.

We were then able to achieve a μ peak value of 0.98 with the following μ -synthesis controller K :

$$K(s) = \frac{-0.07659s^{24} - 5.59s^{23} - 150s^{22} - 1986s^{21} - 1.467 \times 10^4 s^{20} - 6.499 \times 10^4 s^{19}}{s^{25} + 73.85s^{24} + 2022s^{23} + 2.765 \times 10^4 s^{22} + 2.144 \times 10^5 s^{21} + 1.018 \times 10^6 s^{20} \dots} \\ \frac{-1.823 \times 10^5 s^{18} - 3.376 \times 10^5 s^{17} - 4.248 \times 10^5 s^{16} - 3.68 \times 10^5 s^{15} - 2.198 \times 10^5 s^{14} \dots}{\dots 3.132 \times 10^6 s^{19} + 6.521 \times 10^6 s^{18} + 9.466 \times 10^6 s^{17} + 9.745 \times 10^6 s^{16} + 7.159 \times 10^6 s^{15} \dots} \\ \frac{-8.976 \times 10^4 s^{13} - 2.47 \times 10^4 s^{12} - 4542s^{11} - 564.7s^{10} - 48.36s^9 - 2.83s^8 \dots}{\dots 3.74 \times 10^6 s^{14} + 1.375 \times 10^6 s^{13} + 3.503 \times 10^5 s^{12} + 6.12 \times 10^4 s^{11} + 7371s^{10} + 618.6s^9 \dots} \\ \frac{-0.1072s^7 - 0.002189s^6 - 1.526 \times 10^{-5} s^5 - 4.389 \times 10^{-8} s^4 - 5.446 \times 10^{-11} s^3 \dots}{\dots +35.74s^8 + 1.344s^7 + 0.02743s^6 + 0.0001919s^5 + 5.453 \times 10^{-7} s^4 \dots} \\ \frac{-2.484 \times 10^{-14} s^2 - 1.665 \times 10^{-18} s - 2.623 \times 10^{-23}}{\dots 6.574 \times 10^{-10} s^3 + 2.74 \times 10^{-13} s^2 + 1.161 \times 10^{-17} s}$$

The actual μ value is hard to calculate, fortunately J.Doyle had shown that its value lies within an upper and a lower limit. Figure 7.9 shows the μ value limits over the frequency range.

Figure 7.10 shows the response of the closed-loop system when ten different perturbation states are picked randomly using Matlab's *usample* from $G_p(s)$ and an output step disturbance of 10 mOsm/l is applied at time=10 min. The robust performance can be seen by the peak ADH that was of 0.8437, constant in all the ten trials.

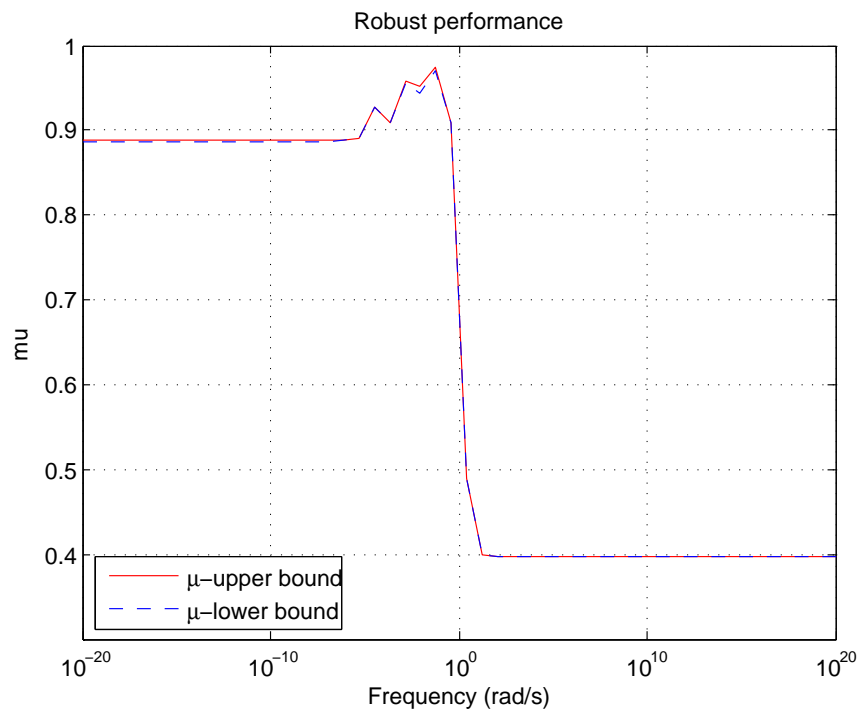


Fig. 7.9 The upper and lower bound of μ , its actual value lies between these upper and lower bounds.

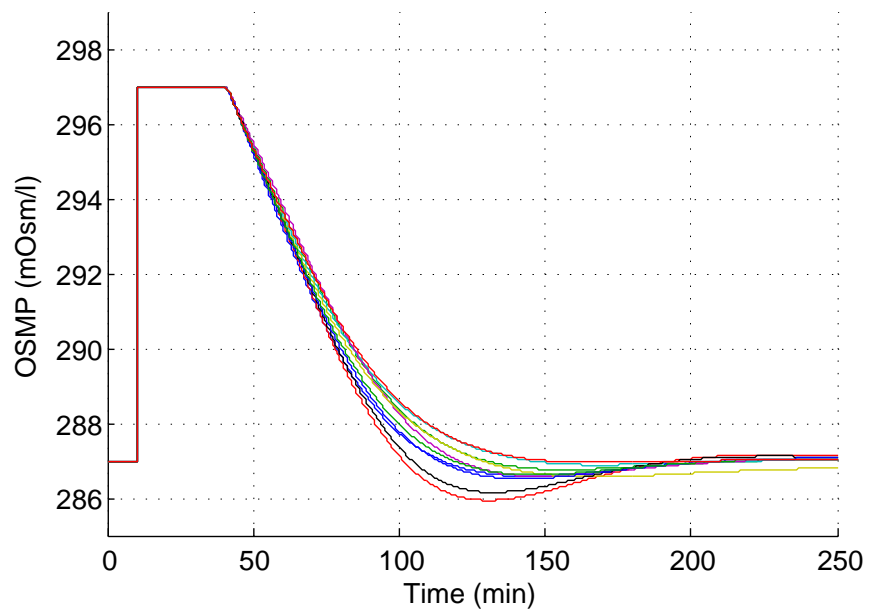


Fig. 7.10 The Osmoregulatory perturbed system's response to a step output disturbance of 10 mOsm/l at time=10 min. 10 different perturbation system's states were picked randomly.

Chapter 8

Conclusion

8.1 Controller's Effectiveness

The human body is an extremely complex biological organism comprising of hundreds of thousands of individual sub-systems, each somehow unique to every one of us. Therefore it was logical to consider a family of osmoregulatory renal systems rather than a nominal one and try to find a controller capable of regulating disturbances in plasma osmolality in those perturbed systems. To study the controllers' performances, we then chose ten different osmoregulatory systems randomly from the family of perturbed ones $G_p(s)$ previously defined and we observed the response of the closed-loop system when those compensators were utilized in rejecting an output step disturbance of 10 mOsm/l. Figure 8.1 shows the responses.

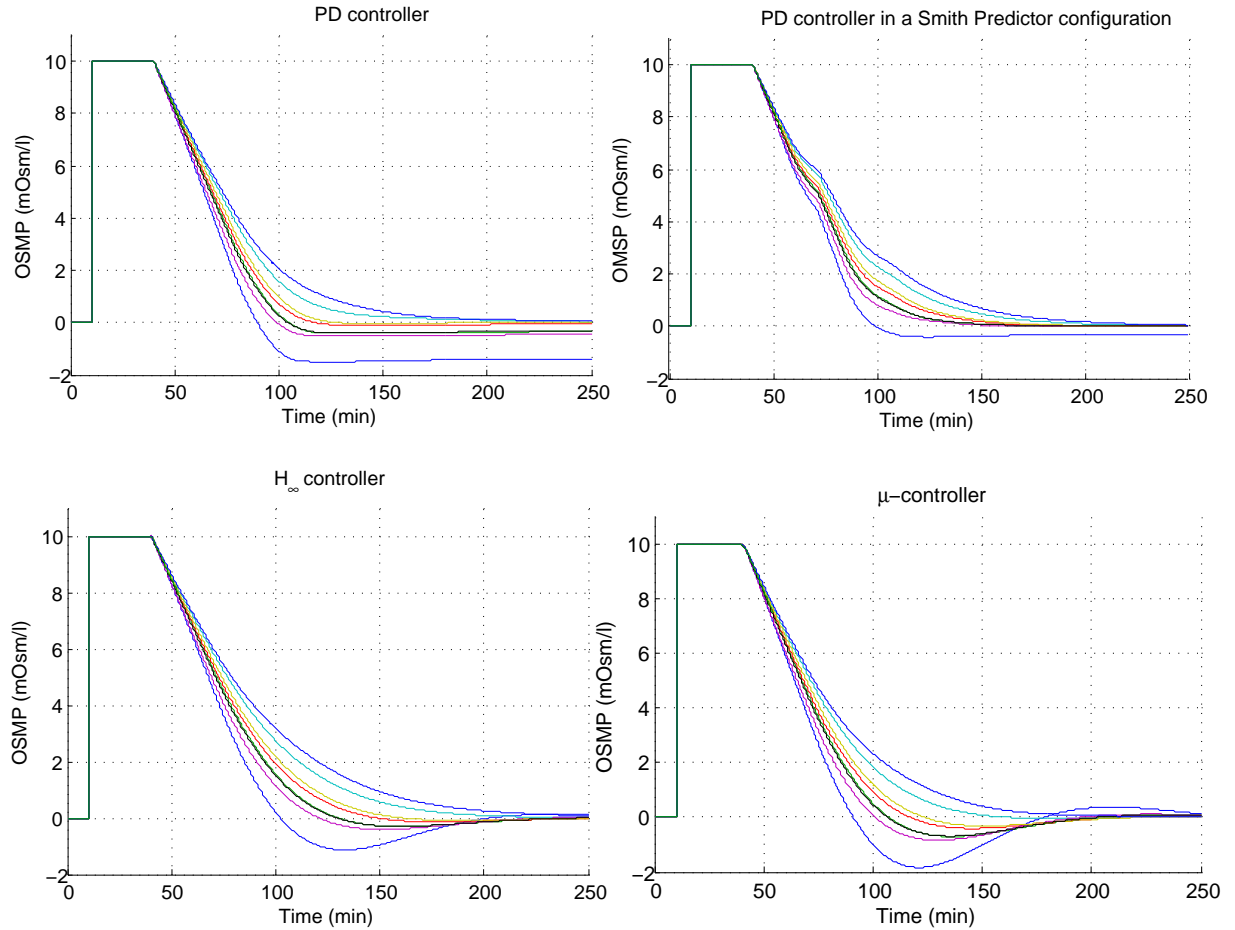


Fig. 8.1 Plots comparing the responses of the osmoregulatory closed-loop system when the four types of controllers are used: PD, PD in a Smith Predictor Configuration, H_∞ Controller and Robust Controller subject to an output step disturbance of 10 mOsm/l. 10 random perturbed model instances are used. These plots represent deviation plots, i.e. 0 mOsm/l is equivalent to 287 mOsm/l.

Table 8.2 shows the settling time¹ of the control system and peak ADH from the controllers' output. When the PD controller (either alone or in a Smith Predictor configuration) is used, a saturation block of 0.8 on the controller's output was used to limit the amount of ADH in the blood stream. In the cases of the \mathcal{H}_∞ Controller and the Robust Controller the ADH was inherently limited to 0.71 and 0.84.

As clearly shown in Table 8.2, in perturbed models 3,4 and 10 the PD controller was never able to achieve $|y(t) - y_{final}(t)| < 0.02$. The same observation could be seen in model 4 with the PD controller in a smith predictor configuration and the \mathcal{H}_∞ optimal controller. Inherently, the Robust controller achieved this criteria in all the 10 perturbed models.

We then removed the saturation blocks and observed the responses (Table 8.3), all controllers except the \mathcal{H}_∞ Controller achieved $|y(t) - y_{final}(t)| < 0.02$.

8.2 Conclusion and Future Work

The objective of this thesis was not to compare the performances of different types of controllers in the purpose of choosing the ultimate best. Depending on the objectives, one might choose one compensator over the other. The PD controller (either alone or in a Smith Predictor configuration), is a simple to design one with appealing characteristics: good performance, ease of tuning and retuning, ease of implementation, vast knowledge in the control community on the subject. As seen in Figure 8.3 the PD controllers performed very well, but the fact that one could not have inherent control over their output may be discouraging to some system designers especially when an upper ADH plasma concentration

¹The Settling Time in this context is defined as the time it takes the error between the actual output $y(t)$ and the desired one $y_{final}(t)$ ($|y(t) - y_{final}(t)|$) to become smaller than a fraction FT of its peak value. FT was chosen here following Matlab's default standard of 0.02 (or 2%).

Perturbed Models	Settling Time			
	PD	SmithPredictor	H_∞	μ -synthesis
1	NaN	115.233	194.2198	180.3422
2	146.1494	164.2703	163.8005	132.2604
3	112.197	150.0661	141.3348	184.1205
4	NaN	NaN	NaN	247.8677
5	NaN	122.3918	187.3287	178.5626
6	106.8337	143.4267	132.2298	180.8396
7	111.2074	148.5965	138.4482	179.5176
8	157.6512	173.0151	171.1591	133.4928
9	NaN	113.5237	191.1769	176.7794
10	NaN	137.6243	184.3341	179.383
Average Settling Time	63.40387	126.81475	150.40319	177.31658

Perturbed Models	Peak ADH			
	PD	SmithPredictor	H_∞	μ -synthesis
1	0.8	0.8	0.7061	0.8437
2	0.8	0.8	0.7061	0.8437
3	0.8	0.8	0.7061	0.8437
4	0.8	0.8	0.7061	0.8437
5	0.8	0.8	0.7061	0.8437
6	0.8	0.8	0.7061	0.8437
7	0.8	0.8	0.7061	0.8437
8	0.8	0.8	0.7061	0.8437
9	0.8	0.8	0.7061	0.8437
10	0.8	0.8	0.7061	0.8437
Average Settling Time	0.8	0.8	0.7061	0.8437

Fig. 8.2 Comparison of the Settling Time and Peak ADH of the osmoregulatory closed-loop system when the four types of controllers are used: PID, PID in a Smith Predictor Configuration, H_∞ Controller and Robust Controller subject to an output step disturbance of 10 mOsm/l. 10 random perturbed model instances are used. When the PID controller either in a Smith Predictor configuration or not is used, a saturation block of 0.8 was added on their output.

limit is required. The \mathcal{H}_∞ Optimal Controller deals with this issue by inherently limiting the controllers output. Unfortunately, the \mathcal{H}_∞ Optimal Controller is highly model based and is not robust to changes in the system's characteristics. The Robust Controller takes the best of both worlds by combining robustness and performance in one controller; However a Robust Controller is harder to design and needs more computing power to run.

Following the investigation done in this thesis, more pertinent projects could follow. In depth work can be done on modeling actual OSMP disturbances in the human body and setting control system objectives in collaboration with a medical group, not only to restore homeostasis but to determine the way in which it has to happen. More research should also be done on building and integrating OSMP sensors in a biological control system environment. Studies on computational speeds and power sources should also be done, if such a device that regulate OSMP in patients with CDI were to be implemented.

Perturbed Models	Settling Time			
	PD	SmithPredictor	H^∞	μ -synthesis
1	112.5421	126.4326	148.4675	158.2122
2	120.2572	123.7447	143.0627	178.5612
3	94.479	138.2062	166.1196	240.4168
4	220.6355	216.5324	NaN	180.3113
5	188.9716	109.4426	192.3137	181.6098
6	188.3606	90.3227	191.545	180.1226
7	166.2636	147.3413	162.4677	180.0611
8	168.9597	114.7181	133.2355	192.2029
9	97.6041	141.7411	170.4815	168.9087
10	122.6514	117.7324	135.7566	171.5746
Average Settling Time	148.0725	132.62141	144.345	183.19812

Perturbed Models	Peak ADH			
	PD	SmithPredictor	H^∞	μ -synthesis
1	3.7	1.7	0.7061	0.8437
2	3.7	1.7	0.7061	0.8437
3	3.7	1.7	0.7061	0.8437
4	3.7	1.7	0.7061	0.8437
5	3.7	1.7	0.7061	0.8437
6	3.7	1.7	0.7061	0.8437
7	3.7	1.7	0.7061	0.8437
8	3.7	1.7	0.7061	0.8437
9	3.7	1.7	0.7061	0.8437
10	3.7	1.7	0.7061	0.8437
Average Settling Time	3.7	1.7	0.7061	0.8437

Fig. 8.3 comparing the Settling Time and Peak ADH of the osmoregulatory closed-loop system when the four types of controllers are used: PID, PID in a Smith Predictor Configuration, \mathcal{H}_∞ Controller and Robust Controller subject to an output step disturbance of 10 mOsm/l. 10 random perturbed model instances are used. No saturation blocks were added in this case.

References

- [1] R. W. Schrier, *Diseases of the Kidney & Urinary Tract*, vol. 11. 8th ed.
- [2] B. M. Koeppen and B. A. Stanton, *Renal Physiology*. Kluwer Academic Publishers, 3rd ed., 2001.
- [3] C. j. LOTE, *Principles of Renal Physiology*. Kluwer Academic Publishers, fourth ed., 2000.
- [4] G. L. Robertson, P. Aycinena, and robert L. Zerbe, “Neurogenic disorders of osmoregulation,” *The American Journal of Medicine*, vol. 72, no. 2, pp. 339 – 353, 1982. Symposium on Disorders of Extracellular Volume and Composition: Part I.
- [5] N. Ikeda, F. Marumo, M. Shirtaka, and T. Sato, “A model of overall regulation of body fluids,” *Annals of Biomedical Engineering*, vol. 7, pp. 135–166, 1979.
- [6] J. B. Jerles and T. Verde, “Air conditioning control system,” Jun 1978.
- [7] U. Kiencke and L. Nielsen, *Automotive Control Systems: For Engine, Driveline, and Vehicle*. Springer, 2nd ed., 2005.
- [8] G. L. Grunkemeier and S. H. Rahimtoola, “Artificial heart valves,” *Annual Review of Medicine*, vol. 41, pp. 251–263, 1990.
- [9] J. E. Youssef, J. Castle, and W. K. Ward, “A review of closed-loop algorithms for glycemic control in the treatment of type 1 diabetes,” *Algorithms*, vol. 2, pp. 518–532, 2009.
- [10] N. Wang, J. Williams, S. Jain, and A. Shalaby, “Post-pacemaker pulsations,” *The American Journal of Medicine*, vol. 122, no. 4, pp. 345–347, 2009.
- [11] B. S. Beckett, *Biology: a modern introduction*. Oxford University Press, 1986.
- [12] D. M. D. for Health Consumers, “Osmole,” 2007.
- [13] G. E. Morgan, M. S. Mikhail, and M. J. Murray, *Clinical anesthesiology*. McGraw-Hill Professional, 2002.

-
- [14] F. Sorrel Greenspan and D. G. Gardner, *Basic and clinical endocrinology*. 7th ed.
- [15] M. P. The MERCK Manuals, the Online Medical Library (reviewed by Ian M. Chapman, “Central diabetes insipidus,” 2002.
- [16] G. R. Del, G. D. Del, C. Marina, A. Roberta, G. G. Del, and V. Mariateresa, “Desmopressin is a safe drug for the treatment of enuresis,” *Scandinavian Journal of Urology and Nephrology*, vol. 39:4, pp. 308–312, 2005.
- [17] D. Segal-Kuperschmit, O. Dali-Gotfrid, and A. Luder, “Water intoxication following desmopressin overdose,” *Harefuah*, pp. 465–467, 1997.
- [18] S. for medical and science inc., “Smsi glucose sensor (in development),” 2009.
- [19] N. MOURLAS, K.H.GILCHRIST, L. GIOVANGRANDI, N. MALUF, and G. KOVACS, “An in-line osmometer for application to a cell-based biosensor system,” *Sensors and actuators. B, Chemical ISSN 0925-4005*, vol. 83, no. 1-3, pp. 41–47, 2002.
- [20] J. Selam and M. Charles, “Devices for insulin administration,” *Diabetes Care*, vol. 13, pp. 955–979, 1990.
- [21] F. Kennedy, “Recent developments in insulin delivery techniques, current status and future potential,” *Drugs*, vol. 42, pp. 213–227, 1991.
- [22] D. Maillefer, H. van Lintel, G. Rey-Mermet, and R. Hirschi, “A high-performance silicon micropump for disposable drug delivery systems,” in *Proceedings of the MEMS 99*, (Orlando, USA), p. 1721 pp. 541546., January 1999.
- [23] A. Guyton, T. G. Coleman, and H. Granger, “Circulation: Overall regulation,” *Ann. Rev. Physiol.*, vol. 34, no. 1, pp. 13–46, 1972.
- [24] R. J. Uttamsingh, M. S. Leaning, J. A. Bushman, E. R. Carson, and L. Finkelstein, “Mathematical model of the human renal system,” *Medical & biological engineering & computing*, vol. 23, no. 6, p. 525, 1985.
- [25] R. Merletti and H. Weed, “Nonlinear model of the body fluid and osmolality control system,” in *Proceedings of the 5th IFAC world congress*, (Paris), pp. 25.1–25.7, 1972.
- [26] G. Ciofani, A. Landi, D. Mazzei, and A. Mazzoldi, “Physiological cybernetics: Model of osmolality and volemia,” in *Proc. IEEE 44th Conference on Decision and Control and the European Control Conference*, (Seville, Spain), pp. 12–15, December 2005.
- [27] D. E. Seborg, T. F. Edgar, and D. A. Mellichamp, *Process Dynamics and Control*. John Wiley and Sons, Inc., 2nd ed., 2003.

-
- [28] O. J. Smith, "A controller to overcome dead time," *ISA Journal*, vol. 6, no. 2, pp. 28–33, 1959.
- [29] D. Leea, M. Leea, S. Sungb, and I. Leeb, "Robust pid tuning for smith predictor in the presence of model uncertainty," *Journal of Process Control*, vol. 9, no. 1, pp. 79–85, 1999.
- [30] P. Chandrasekharan, *Robust Control of Linear Dynamical Systems*. Academic Press, 1996.
- [31] J. S. Freudenberg, D. Looze, and J. Cruz, "Robustness analysis using singular value sensitivities," *Int. J. Contr.*, vol. 35, pp. 95–116, 1982.
- [32] M. Safonov, "bounds on the response of multivariable systems with component uncertainty," *Allerton Conference on Communication, Control and Computing*, pp. 451–460, 1978.
- [33] J. Doyle, "Analysis of feedback systems with structured uncertainties," *IEE Proceedings*, vol. 129, no. 6, pp. 242–250, 1982.
- [34] S.Koshikawa and K. Suzuki, "Study of osmo-regulation as feedback system," *Med. & biol. Engng.*, vol. 6, pp. 149–158, 1968.
- [35] E. T. R. H. L. W. L. BARBARA J. ROLLS, R. J. WOOD and J. G. G. LEDINGHAM, "Thirst following water deprivation in humans," *Regulatory, Integrative and Comparative Physiology*, vol. 239, no. 5, pp. 476–482, 1980.
- [36] R. G. Ralf Keil and E. Simon, "Effects of changes in intravascular oncotic pressure on renal responses to volume loading in the saltwater-acclimated pekin duck (*anas platyrhynchos*)," *Journal of Comparative Physiology*, vol. 161, pp. 179–187, 1991.
- [37] H. kwakernaak, "Robust control and h_∞ -optimization-tutorial paper," *Automatica*, vol. 29, no. 2, pp. 255–273, 1993.
- [38] K. Zhou and J. Doyle, *Essentials of robust control*. Prentice Hall, 1998.